의학박사 학위논문

Anti-aging effects of plant extracts on skin and brain in hairless mice

각종 식물추출물이 무모쥐의 피부 및 뇌기능의 노화에 미치는 영향

2017 년 2 월

서울대학교 대학원

의과학과 의과학전공

배 정 수

각종 식물추출물이 무모쥐의 피부 및 뇌기능의 노화에 미치는 영향

지도교수 정 진 호

이 논문을 의학박사 학위논문으로 제출함

2017 년 2 월

서울대학교 대학원

의과학과 의과학전공

배 정 수

배정수의 의학박사 학위논문을 인준함

2017 년 2 월

위 원 장 _____ (인)

부위원장 _____ (인)

위 원 _____ (인)

위 원 _____ (인)

위 원 _____ (인)

Anti-aging effects of plant extracts on skin and brain in hairless mice

by

Bae Jung-Soo

A thesis submitted to the Department of Biomedical Science in partial fulfillment of the requirements for the Degree of Doctor of Philosophy in Biomedical Science at Seoul National University College of Medicine

February 2017

Approved by Thesis Committee:

Professor _____ **Chairman**

Professor _____ **Vice chairman**

Professor _____

Professor _____

Professor _____

ABSTRACT

Aging is a natural process with the passage of time. As aging progresses, the body changes externally and internally, with a decline in organ function. These changes occur primarily in the skin and brain. Reduced water retention and increased wrinkle formation are the most common phenotypes of aged skin. In case of the brain, cognitive deficits and memory impairment occur in a large number of the elderly populations. Lots of aged populations desire to be rejuvenated for maintaining a healthy body.

In this study, I tried to find out anti-aging agents especially those that affect skin and brain functions by using 133 ethanolic extracts of dietary plants. Extracts of two plant species were selected for being protective against skin and brain aging, respectively.

Perilla frutescens (L.) Britt. (Lamiaceae) is an herb used as a food and a traditional medicine in Korea. In this study, *P. frutescens* leaf extract (PLE) significantly inhibited basal and UV-induced matrix metalloproteinase-1 (MMP-1) expression in a dose-dependent manner, and promoted type I procollagen production irrespective of UV irradiation. The inhibitory effect of PLE on MMP-1 expression was mediated by inhibition of ROS/mitogen-activated protein kinase (MAPK)/AP-1 signaling pathway. Furthermore, PLE significantly

reduced epidermal skin thickness and MMP-13 expression induced by UV in a UV-irradiated animal model.

Tomato (*Lycopersicon esculentum*) is consumed worldwide as fruit, and is also known as a super food because of their many physiological activities. In this study, oral administration of tomato ethanolic extracts (TEE) for 6 weeks significantly increased the exploration time of novel objects, proliferation of hippocampal cells, and synaptic plasticity in 12-month-old mice compared to those in vehicle-treated aged mice. The memory enhancing effect of the TEE treatment resulted from an increased expression of brain-derived neurotrophic factor (BDNF) and the subsequent activation of ERK/CREB signaling pathway in the hippocampus.

In conclusion, the selected antiaging agents, PLE and TEE, showed an anti-aging effect on the skin by inhibition of the ROS/MAPK/AP-1 pathway and on the brain by the BDNF/ERK/CREB pathway. These results suggest that PLE and TEE can be potential agents for prevention of skin aging and treatment of age-related memory impairment and neurodegenerative disorders.

Keywords: Aging, plant extract, MMP, collagen, neurodegeneration, BDNF, cognitive function

Student Number: 2011-30629

CONTENTS

LIST OF TABLES

Chapter I

LIST OF FIGURES

Chapter I

Chapter II

Chapter II

GENERAL INTRODUCTION

Photoaging

Skin exposure to ultraviolet (UV) radiation causes DNA damage, alterations in cellular components, and degradation of extracellular matrix (ECM) components including collagen and elastin fibers in the dermis [1]. Matrix metalloproteinases (MMPs) are zinc-dependent endopeptidases and important in the remodeling of ECM structure in skin. Among the MMPs, MMP-1 and MMP-3 (collagenase) are responsible for diverse physiologic processes, such as development and tissue morphogenesis [2,3]. Type I collagen is the most dominant component of the dermis ECM with an important role in the maintenance of skin structure [4]. Skin exposure to UV radiation is known to increase the expression of MMP-1 and suppress the synthesis of type I collagen [5].

UV irradiation induces the generation of reactive oxygen species (ROS), and subsequently activates the mitogen-activated protein kinase (MAPK) signaling cascade [6,7]. This ROS/MAPK signaling pathway activation increases the transcriptional activity of the activator protein-1 (AP-1) complex. The activated AP-1 is responsible for the

degradation of collagen by inducing MMP-1, MMP-3, and MMP-9 [8,9]. Several specific MAPK inhibitors are reported to effectively protect against UV-mediated damage. Thus, inhibition of the MAPK cascade has been considered as a therapeutic target against photoaging.

.

Brain aging and neurodegeneration

Neurogenesis is the overall process of generation of neurons from neural stem cells and progenitor cells, and the subgranular zone (SGZ) in the hippocampus is a major brain region involved in adult neurogenesis [10]. Neurogenesis is most active during prenatal development and declines substantially with age [11]. Neurodegeneration is a notable phenomenon of aging. A large number of the elderly suffer from cognitive deficits, such as memory impairment, Alzheimer's disease, and depression [12]. The hippocampus plays an important role in learning and memory; however, its function and histologic integrity deteriorate with age [13]. There is considerable histologic evidence of brain aging such as hippocampal atrophy and synaptic degeneration [14]. Thus age-related hippocampal deterioration can be considered a cause of memory decline.

The brain is known to be influenced by several hormones and growth factors that affect the generation, maturation, and survival of neurons [15], however, levels of most neurotrophic factors decline with

age. For this reason, considerable efforts have been made to increase levels of age-decreased neurotrophic factors such as the nerve growth factor (NGF) and brain-derived neurotrophic factor (BDNF) [16,17].

BDNF is a well-known neurotrophic factor that regulates not only the growth and differentiation of newborn neurons but also synaptic plasticity via activation of signaling pathways involved in the release of neurotransmitters [18]. It has been reported that BDNF induces hippocampal neurogenesis and assists memory formation by activation of extracellular-signal-regulated kinase 1/2 (ERK1/2)/cAMP response element binding (CREB) signaling pathway [19]. Therefore, BDNF is a potent therapeutic target to improve memory.

CHAPTER I

Screening of agents for protecting skin and brain aging

INTRODUCTION

Plants have been used as a natural source of pharmaceutical agents. For example, flavonoids are found in various kinds of plants as plant pigments, and have many pharmacological activities such as antioxidant, anti-inflammatory, and anticancer effects. Resveratrol is also a well-known pharmaceutical agent extracted from the skin of grapes, blueberries, and raspberries that has cardioprotective, anti-diabetic, skin protective, and anticancer activities. Besides, genistein, carotenoids, and curcumin are noted efficacious phytochemicals. In addition, there are several popular drugs that have been developed either directly or indirectly from plant ingredients. Despite numerous drugs that have been derived from plants until now, a large number of studies to find novel drugs from plants are performing actively because of their potential.

The purpose of the study described in this chapter was to find out putative antiaging agents with skin and brain benefits for an efficacy study. To find such agents, 133 commonly consumed dietary plants were extracted using a 50%-ethanol extraction method, and used for the

screening of antiaging agents.

METERIALS AND METHODS

Preparation of plant ethanolic extracts

Commonly consumed dietary plants were provided by Korea Food Research Institute (Seongnam-si, Korea). Specifically, 133 kinds of plants were shade-dried, powdered, and sequentially extracted with 50% ethanol using a microwave system for 5 min at 55-59^{o}C. The extract was filtered and freeze-dried at -40°C under reduced pressure.

Materials

Bromodeoxyuridine (BrdU) was purchased from Sigma (St. Louis, MO, USA). The antibodies used in this study were as follows; rabbit polyclonal antibodies against MMP-1 (Lab Frontier, Seoul, Korea), type I procollagen (SP1.D8) (Developmental Studies Hybridoma Bank, Iowa City, IA, USA), goat polyclonal antibodies against DCX (sc-8066, Santa Cruz Biotechnology, Santa Cruz, CA, USA), rabbit polyclonal antibodies against Ki-67 (KCL-Ki67p, novocastra, Newcastle, UK), rat monoclonal antibodies against BrdU (YSRTMCA2060GA, Accurate Chemical, Westbury, NY)

Cell culture

Primary human dermal fibroblasts (HDFs) were isolated from foreskin of young volunteers aged 10-19 years and cultured in Dulbecco's modified Eagle's media (DMEM; Gibco-BRL, Carlsbad, CA, USA), supplemented with 10% fetal bovine serum (FBS; Gibco-BRL) and penicillin/streptomycin (400 U/mL, 50 g/L) at 37°C in a humidified condition with 5% CO_2.

Western blot analysis

Western blot analysis was performed as described previously [20]. HDFs were lysed with 50 mM Tris-HCl (pH 7.4) buffer with protease inhibitor and phosphatase inhibitor cocktails (Sigma-Aldrich, St. Louis, MO). Protein quantities of cell lysates were determined using BCA reagent (Sigma-Aldrich). Equal amounts of protein was separated by SDS-polyacrylamide gel electrophoresis, and then transferred to PVDF membrane (Amersham, Buckinghamshire, UK). The membrane was blocked in 5% skim milk in TBST and incubated with primary antibodies. The blots were further incubated with horseradish peroxidase-conjugated secondary antibody. Blotting protein were visualized using an ECL detection system (GE Healthcare, UK).

Reverse transcription and real-time quantitative PCR

Total RNA was isolated from HDFs using RNAiso Plus (Takara Bio Inc., Shiga, Japan) as previously described [21]. cDNAs were synthesized from isolated RNA templates using a First Strand cDNA Synthesis Kit (MBI Fermentas, Vilnius, Lithuania). The cDNAs were subject to quantitative PCR. PCR products was quantitated by 7500 Real time PCR System (Applied Biosystems, Foster City, CA, USA) with SYBR Premix Ex Taq II kit (Takara Bio). The PCR reactions were performed with the following primers; BDNF, IGF-1, FGF-2 and endogenous reference 36B4. Data were analyzed using the $2^{-\Delta\Delta CT}$ methods and expressed as fold changes of gene expression relative to 36B4.

Treatments for neurotrophic factors.

Seven-week-old female albino hairless mice (Skh-1) were obtained from Orient Bio Inc. (Seoul, Korea). Animals were acclimated for 1 week prior to the study and had free access to food and water. All experimental protocols were approved by the Institutional Animal Care and Use Committees (IACUC No. 14-008-S1A0) at Seoul National University. Mice were injected 100mg/Kg/day of BrdU for 2day intraperitoneal. After BrdU injection, mice were treated with neurotrophic factors by subcutaneous injection for every 14 days. Each

group composed of six mice and mice treated with vehicle were used as positive control.

Treatments for plant ethanolic extracts.

Eighteen-year-old female albino hairless mice (Skh-1) were obtained from Orient Bio Inc. (Seoul, Korea). Animals were allowed to feed *ad libitum*, and acclimated for 1 week prior to the study. All experimental protocols were approved by the Institutional Animal Care and Use Committee of Center for Phenogenomics Animal Research Facility, Woojung BSC (Suwon, Korea, Association for Assessment and Accreditation of Laboratory Animal Care-accredited facility). The aged mice were randomly divided into seven equivalent groups (n=6) : those with vehicle or turmeric, aster scaber, tomato, broccoli, proso millet and lemon extracts administration. The animals were orally fed with a dose of 400 mg/kg using a feeding needle once daily for 4 weeks, and 0.5% carboxymethyl cellulose-sodium solution was used as vehicle.

Immunohistochemistry

Immunostaining was performed using the free floating technique. One series was randomly selected, and stained using antibodies. For BrdU labeling, Mice were administered BrdU (100 mg/kg) by intraperitoneal injections for 2 day, and brain sections were incubated

with 2N HCl for 30 min, and neutralized by boric acid for 10 min. After blocking with Ultra-V block (Lab Vision, Fremont, CA), The free floating slices were incubated for 2 days at 4°C with the primary antibodies in a diluent buffer (1% bovine serum albumin (BSA) and 1% Triton X-100 in 0.1 M phosphate buffer). Subsequently, sections were incubated for 24h at 4°C with Alexa Fluor 488-conjugated secondary antibody (Invitrogen, Camarillo, CA, USA). For BrdU labeling, Mice were administered BrdU (100 mg/kg) by intraperitoneal injections for 2 days.

Quantitation of fluorescent-labeled cells

The images were taken with a Leica DM5500B microscope (Leica). To quantify the total cell number of fluorescent-labeled cells in the SGZ, all sections were coded and cell counting was performed with the examiner blinded to group allocation.

Statistical analysis

All data were analyzed using SPSS software (IBM, Armonk, NY, USA). Results are expressed as means±SEM, and statistical analyses were performed using Mann-Whitney test. *P*-values of less than 0.05 were considered statistically significant.

RESULTS

Preparation of plant ethanolic extracts

To prepare plant extracts for the screening of anti-aging effects, 133 kinds of commonly consumed dietary plants categorized by types of roots (3 species), nuts (13 species), grains (11 species), fruits (24 species), mushrooms (7 species), beens (6 species), vegetables (63 species) and seaweeds (6 species) were selected, and subjected to the screening study. Dietary plants used in this study were purchased from korea traditional market, and extracted by 50% ethanol using microwave system. **Table 1** shows the extraction yields for the plant extracts. The extraction yields varied from 0.55% to 64.04%.

Screening of anti-aging agents for skin

To find out effectual plant extracts for regulating expressions of

MMP-1 and procollagen, HDFs were seeded and treated with 100μg/ml of plant extracts for 48 h after UV. To evaluate effects of plant extracts on expressions of MMP-1 and procollagen, cell culture supernatants were analyzed by Western blotting. **Figure 1** shows expressions of MMP-1 and procollagen regulated by plant extracts. Total 13 species of extracts inhibited UV-induced MMP-1 expression without the reduction of UV-reduced procollagen expression. Especially, 3 species of extracts not only inhibited UV-induced MMP-1 expression, but also increased UV-reduced procollagen expression.

Subcutaneous administration of BDNF, FGF-2, IGF-1 and DHEA increased hippocampal neurogenesis in Skh-1 hairless mice

To investigate whether peripheral neurotrophic factors can increase hippocampal neurogenesis, BDNF (267ug/Kg/day), FGF-2 (30ug/Kg/day), IGF-1 (3mg/Kg/day) and DHEA (40mg/Kg/day) were injected subcutaneously for 14 days, and overall cell proliferation and survival in the SGZ of dentate gyrus (DG) was assessed by immunohistochemistry for Ki67 (a marker for immature neurons) and BrdU, respectively. It was demonstrated that mice injected with all peripheral neurotrophic factors showed a significant increase in the numbers of Ki-67^{+} cells in DG compared with vehicle-treated mice (**Figure 2A)**. Furthermore, subcutaneous administration of most

peripheral neurotrophic factors, except BDNF, significantly induced neuronal cell survival (**Figure 2B)**. These findings suggest that peripheral increase of BDNF, FGF-2, IGF-1 and DHEA can induce hippocampal neurogenesis in mice.

Screening of anti-aging agents for brain in HDFs

To find out effective plant extracts increasing peripheral neurotrophic factors, HDFs were treated with 100μg/ml of plant extracts for 6 h, and mRNA expressions of BDNF, FGF-2 and IGF-1 were analyzed by real-time PCR. **Figure 3** shows mRNA expressions of BDNF regulated by plant extracts. Total 7 species of extracts increased of BDNF mRNA expressions more than 2 folds compared with control. **Figure 4** shows mRNA expressions of FGF-2 regulated by plant extracts. Total 17 species of extracts increased of BDNF mRNA expressions more than 3 folds compared with control. **Figure 5** shows mRNA expressions of IGF-1 regulated by plant extracts. Total 4 species of extracts increased of BDNF mRNA expressions more than 2 folds compared with control. From the screening using HDFs, Total 22 species of extracts were selected as putative agents enhancing neurotrophic factors.

Screening of anti-aging agents for brain in Skh-1 hairless mice

To find out effective plant extracts increasing hippocampal

neurogenesis, 400mg/kg/day of 6 species of plant extracts (finally selected *in vitro* model) were orally administrated in Skh-1 hairless mice for 4 weeks. Overall cell proliferation in the SGZ of DG was assessed by immunohistochemistry, and Ki-67 and DCX were used as markers for hippocampal neurogenesis. It was demonstrated that oral administration of tomato extract results in a significant induction by 1.44-fold in the number of Ki-67^{+} cells in DG compared with vehicle-treated mice (100.0±10.34 vs. 144.3±12.75; vehicle vs. TEE) (**Figure. 6**). In addition, oral administration of tomato and proso millet also showed a significant increase (1.64-fold) in the numbers of DCX^{+} cells in DG compared with vehicle-treated mice (**Figure 7)** (100.0±6.58 vs. 163.5±18.83; vehicle vs. TEE). These findings suggest that tomato and proso millet has a putative effects protecting aging of brain.

Table 1. List of plant ethanolic extracts

Korean Name	Scientific name	Yield(%, w/w)	Korean Name	Scientific name	Yield(%, w/w)
가지	Solanum melongena	**3.28**	통밀	Triticum spp seeds	**4.38**
근대	Beta vulgaris	**3.08**	쌀보리	Hordeum vulgare seeds	**3.63**
단호박	Cucurbita maxima	**8.46**	두부	Tofu	**1.44**
달래	Allium monanthum	**8.79**	순부부	Soft tofu	**2.35**
당근	Daucus carota	**6.96**	밤	Castanea crenata nuts	**9.8**
더덕	Codonopsis lanceolata	**13.84**	밤껍질	Castanea crenata nutshell	**7.04**
도라지	Platycodon grandifloras	**5.45**	은행	Ginkgo biloba nuts	**5.46**
돌나물	Sedum sarmentosum	**1.73**	잣	Pinus koraiensis nuts	**14.31**
들깻잎	Perilla frutescens Leaves	**3.11**	땅콩	Arachis hypogaea nuts	**6.58**
마늘	Allium scorodorpasum	**28.01**	느타리버섯	Pleurotus ostreatus	**5.85**
무	Raphanus raphanistrum subsp	**2.69**	송이버섯	Tricholoma matsutake	**5.91**
무순	Raphanus raphanistrum subsp sprouts	**1.59**	양송이버섯	Agaricus bisporus	**4.64**
미나리	Oenanthe javanica	**3.07**	새송이버섯	Pleurotus eryngii	**6.63**
부추	Allium tuberosum	**3.54**	팽이버섯	Flammulina velutipes	**5.53**
붉은고추	Capsicum annuum(red)	**8.2**	표고버섯	Lentinula edodes	**7.98**
브로콜리	Brassica oleracea	**6.44**	목이버섯	Auricularia auricula-judae	**0.55**
상추	Lactuca sativa	**2.54**	단감	Diospyros kaki fruits	**12.1**
생강	Zingiber officinale	**2.18**	귤	Citrus unshiu flesh	**10.29**
샐러리	Apium graveolens	**2.94**	대추	Zizyphus jujuba var. inermis fruits	**32.37**
숙주나물	Vigna radiata sprouts	**2.25**	망고	Mangifera indica fruits	**11.46**
시금치	Spinacia oleracea	**6.04**	무화과	Ficus carica fruits	**39.66**
신선초(명일엽)	Angelica keiskei	**3.86**	바나나	Musa × paradisiaca fruits	**17.51**
쑥갓	Chrysanthemum coronarium	**1.48**	오렌지	Citrus X sinensis fruits	**12.88**
파프리카	Capsicum frutescens	**5.9**	키위	Actinidia chinensis fruits	**10.7**
피망	Capsicum annuum var. angulosum	**3.12**	포도	Vitis vinifera L. fruits	**10.85**
감자	Solanum tuberosum	**3.42**	찰수수	Sorghum bicolor	**1.41**
자색고구마	Ipomoea batatas	**7.54**	흑미	Oryza sativa L seeds (black rice)	**2.68**
풋고추	Capsicum annuum(green)	**2.63**	현미	Oryza sativa L seeds (brown rice)	**1.91**
고춧잎	Capsicum annuum leaves	**14.31**	찹쌀	Oryza sativa var. glutinosa seeds	**0.59**
곰취	Ligularia fischeri	**3.43**	메조	Setaria italic seeds	**2.1**
냉이	Capsella bursa-pastoris	**6.63**	율무	Coix lacryma-jobi	**1.83**
머위	Petasites japonicus	**2.5**	기장	Panicum miliaceum seeds	**1.89**
배추	Brassica rapa subsp. pekinensis	**3.64**	녹두	Vigna radiate seeds	**9.2**
비트	Beta vulgaris	**12.53**	검정콩	Phaseolus vulgaris 'Black turtle	**13.91**

Korean Name	Scientific name	Yield(%, w/w)	Korean Name	Scientific name	Yield(%, w/w)
쑥	Artemisia princeps	**10.11**	약콩	Glycine max seeds	**12.68**
야콘	Smallanthus sonchifolius roots	**15.15**	들깨	Perilla frutescens seeds	**13.35**
원추리	Hemerocallis fulva	**3.96**	아몬드	Prunus dulcis nuts	**5.62**
유채	Brassica napus leaves	**3.99**	검정참깨	Sesamum heukimja seeds	**5.98**
참나물	Pimpinella brachycarpa	**2.61**	흰참깨	Sesamum indicum seeds	**6.3**
취나물	Aster scaber	**4.93**	호두	Juglans regia nuts	**24.73**
방울토마토	Solanum lycopersicum var. cerasiforme	**4.18**	해바라기씨	Helianthus annuus seeds	**8.94**
대파	Allium fistulosum	**6.86**	호박	Cucurbita moschata seeds	**12.36**
둥글레	Polygonatum odoratum var. Pluriflorum roots	**53.3**	피스타치오넛	Pistacia vera nuts	**9.35**
배추시래기	Brassica rapa var. Glabra dried Leaves	**3.6**	토마토	Solanum lycopersicum	**3.64**
토란대	Colocasia esculenta stem	**2.55**	자몽	Citrus maxima fruits	**9.34**
고사리	Pteridium aquilinum	**12.96**	레몬	Citrus × limon fruits	**6.68**
아욱	Malva verticillata	**2.14**	건포도	Vitis vinifera dried fruits	**64.04**
알로에	Aloe spp	**1.69**	한라봉	Citrus reticulata 'Shiranui' fruits	**12.47**
애호박	Cucurbita pepo var. cylindrical	**4.11**	귤과피	Citrus unshiu skin	**11.4**
양배추	Brassica oleracea var. capitata	**5.27**	오렌과피	Citrus X sinensis skin	**9.16**
양상추	Lactuca sativa	**2.78**	자몽과피	Citrus maxima skin	**6.68**
양파	Allium cepa	**5.18**	레몬과피	Citrus × limon skin	**6.3**
연근	Nelumbo nucifera	**4.6**	한라봉과피	Citrus reticulata 'Shiranui' skin	**11.88**
열무	Raphanus sativus L.	**2.46**	백미	Oryza sativa L seeds (white rice)	**0.71**
오이	Cucumis sativus	**1.51**	참마 (산마)	Dioscorea japonica roots	**3.26**
우엉	Arctium lappa	**14.11**	팥	Vigna angularis seeds	**7.42**
쪽파(골파)	Allium wakegi Araki	**3.67**	갓	Brassica juncea	**3.57**
청경채	Brassica rapa var. Chinensis	**2.76**	석류	Punica granatum fruits	**11.74**
치커리, 녹색잎	Cichorium intybus Leaves	**2.26**	파인애플	Ananas comosus fruits	**13.85**
컬리플라워	Brassica oleracea var. botrytis	**4.51**	김	Pyropia tenera	**9.5**
케일	Brassica oleracea var. sabellica	**3.32**	매생이	Capsosiphon fulvescens	**4.28**
콩나물	Glycine max sprout	**2.15**	미역	Undaria pinnatifida	**4.64**
파슬리	Petroselinum crispum	**5.14**	톳	Sargassum fusiforme	**6.27**
딸기	Fragaria × ananassa	**7.81**	파래	Enteromorpha	**3.79**
배	Pyrus fruits	**10.66**	감태	Ecklonia cava	**3.58**
사과	Malus domestica fruits	**14.67**	귤(과육,과피)	Citrus unshiu flesh and skin	**10.91**
메밀	Fagopyrum esculentum seeds	**2.75**			

Figure. 1.

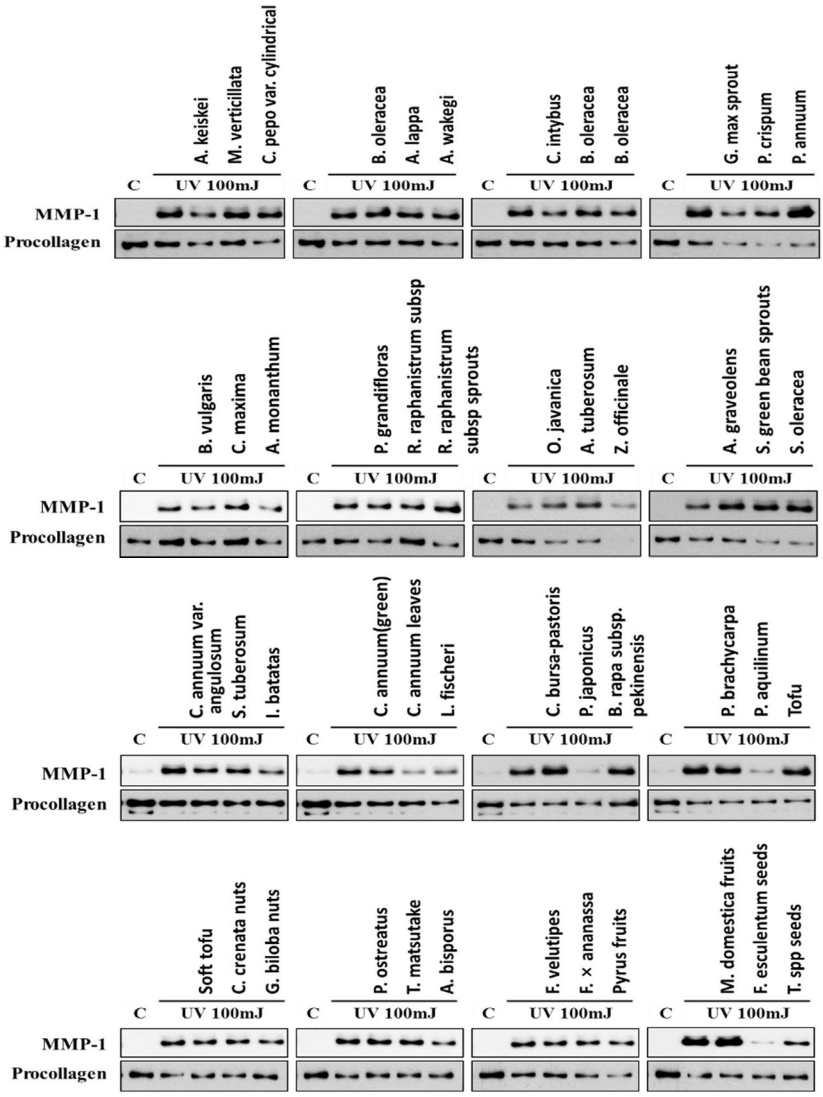
C
UV 100mJ
MMP-1
Procollagen
A. keiskei
M. verticillata
C. pepo var. cylindrical
B. oleracea
A. lappa
A. wakegi
C. intybus
B. oleracea
B. oleracea
G. max sprout
P. crispum
P. annuum
B. vulgaris
C. maxima
A. monanthum
P. grandifloras
R. raphanistrum subsp
R. raphanistrum subsp sprouts
O. javanica
A. tuberosum
Z. officinale
A. graveolens
S. green bean sprouts
S. oleracea
C. annuum var. angulosum
S. tuberosum
I. batatas
C. annuum(green)
C. annuum leaves
L. fischeri
C. bursa-pastoris
P. japonicus
B. rapa subsp. pekinensis
P. brachycarpa
P. aquilinum
Tofu
Soft tofu
C. crenata nuts
G. biloba nuts
P. ostreatus
T. matsutake
A. bisporus
F. velutipes
F. × ananassa
Pyrus fruits
M. domestica fruits
F. esculentum seeds
T. spp seeds

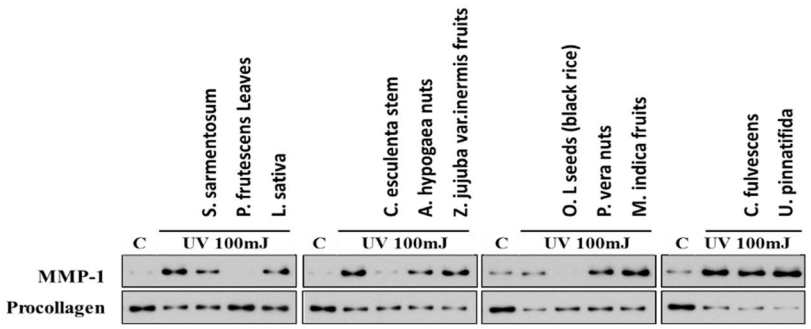

Figure 1. Screening of plant ethanolic extracts for regulating expressions of MMP-1 and procollagen in HDFs

HDFs were irradiated with 100 mJ/cm^2 of UV and treated with diverse plant ethanolic extracts for 48 h. Culture media was harvested and MMP-1 and procollagen expression were measured by western blotting.

Figure. 2.

A

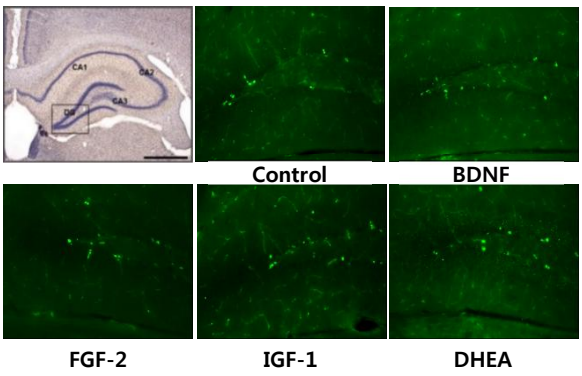
Control
BDNF
FGF-2
IGF-1
DHEA

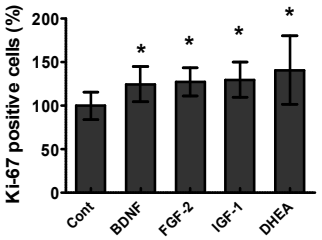
Ki-67 positive cells (%)
200
150
100
50
0
*
*
*
*
Cont
BDNF
FGF-2
IGF-1
DHEA

B

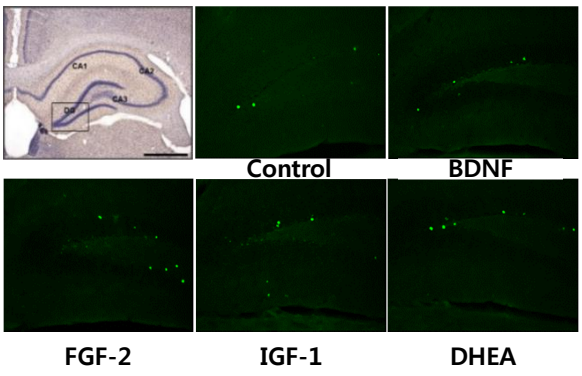
Control
BDNF
FGF-2
IGF-1
DHEA

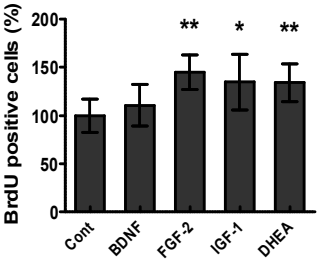
BrdU positive cells (%)
200
150
100
50
0
**
*
**
Cont
BDNF
FGF-2
IGF-1
DHEA

Figure 2. Effect of subcutaneous injection of neurotrophic hormones on hippocampal neurogenesis and neuronal cell survival in Skh-1 hairless mice.

To evaluate effects of neurotrophic hormones on hippocampal neurogenesis and neuronal cell survival in DG, mice were 100mg/Kg/day of BrdU was administrated by intraperitoneal injections. After 2 days of BrdU injection, mice were injected with BDNF, FGF-, IGF-1 and DHEA subcutaneously for 14 days, and immunostaining was performed using antibodies against DCX and BrdU. (A) Representative photographs of DCX^+ cells in hippocampal were shown. Total number of DCX^+ cells in the DG were quantified in the graph in the right panel. (B) Representative photographs of $BrdU^+$ cells in hippocampal were shown. Total number of $BrdU^+$ cells in the DG were quantified in the graph in the right panel. Each bar represents mean±SEM of each group (n=6). Asterisks denote significant difference (*, $P < 0.05$; **, $P < 0.01$).

Figure. 3.

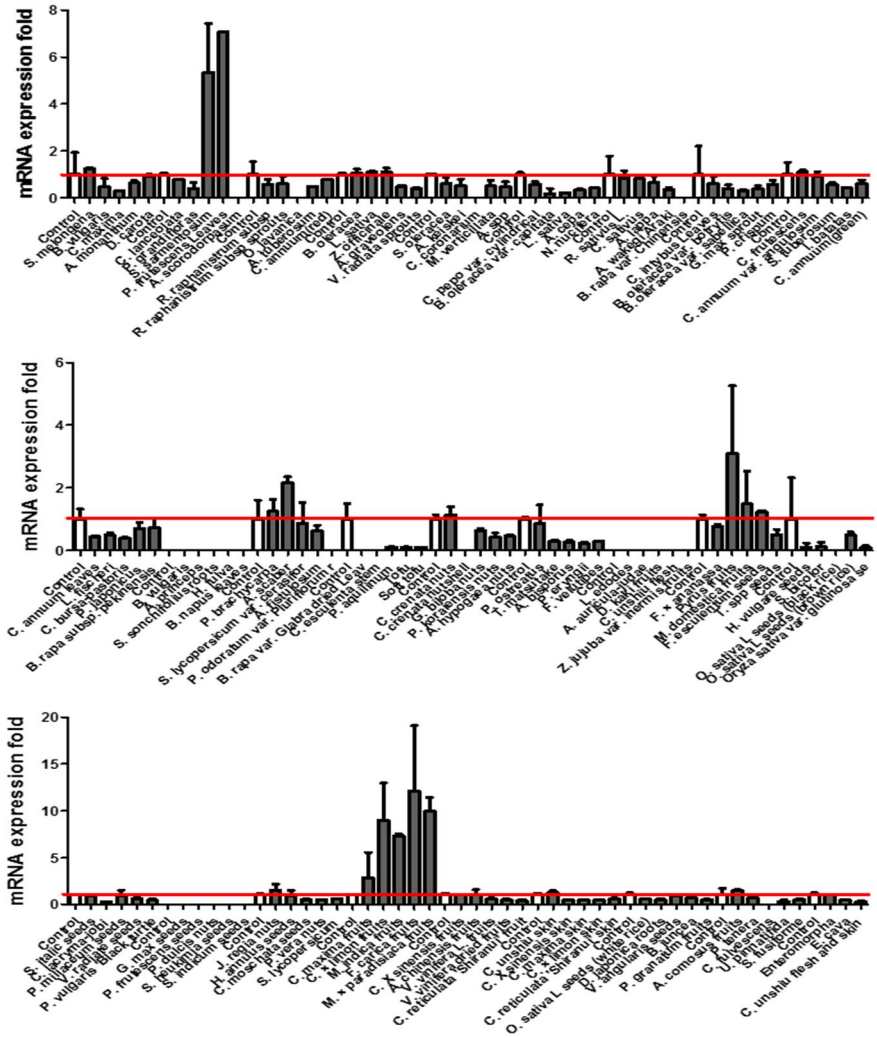

Figure 3. Screening of plant ethanolic extracts for activating BDNF

mRNA expression.

HDFs were treated with diverse plant ethanolic extracts. After incubation for 6 h, cells were harvested and mRNA levels of BDNF were determined by RT-qPCR. All RT-qPCR experiments were performed two times. Each bar represents the mean ± SEM.

Figure. 4

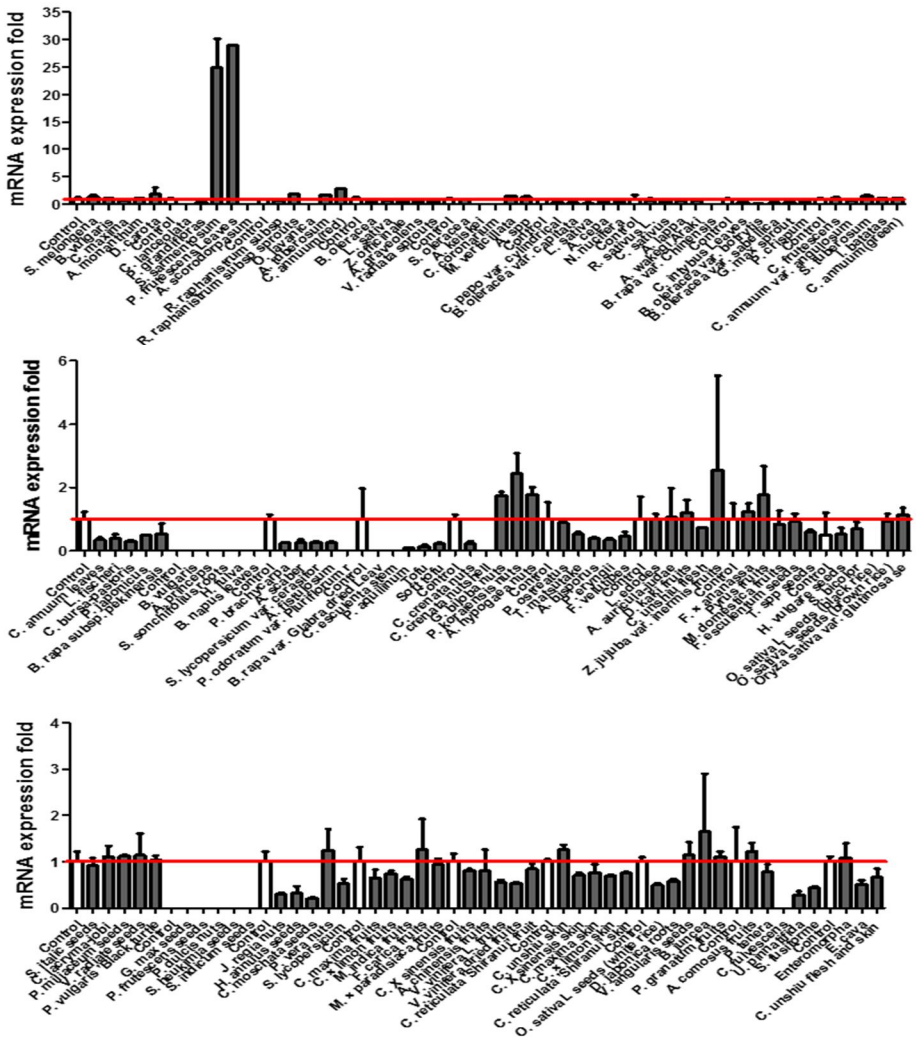

Figure 4. Screening of plant ethanolic extracts for activating FGF-2

mRNA expression.

HDFs were treated with diverse plant ethanolic extracts. After incubation for 6 h, cells were harvested and mRNA levels of IGF-2 were determined by RT-qPCR. All RT-qPCR experiments were performed two times. Each bar represents the mean ± SEM.

Figure. 5

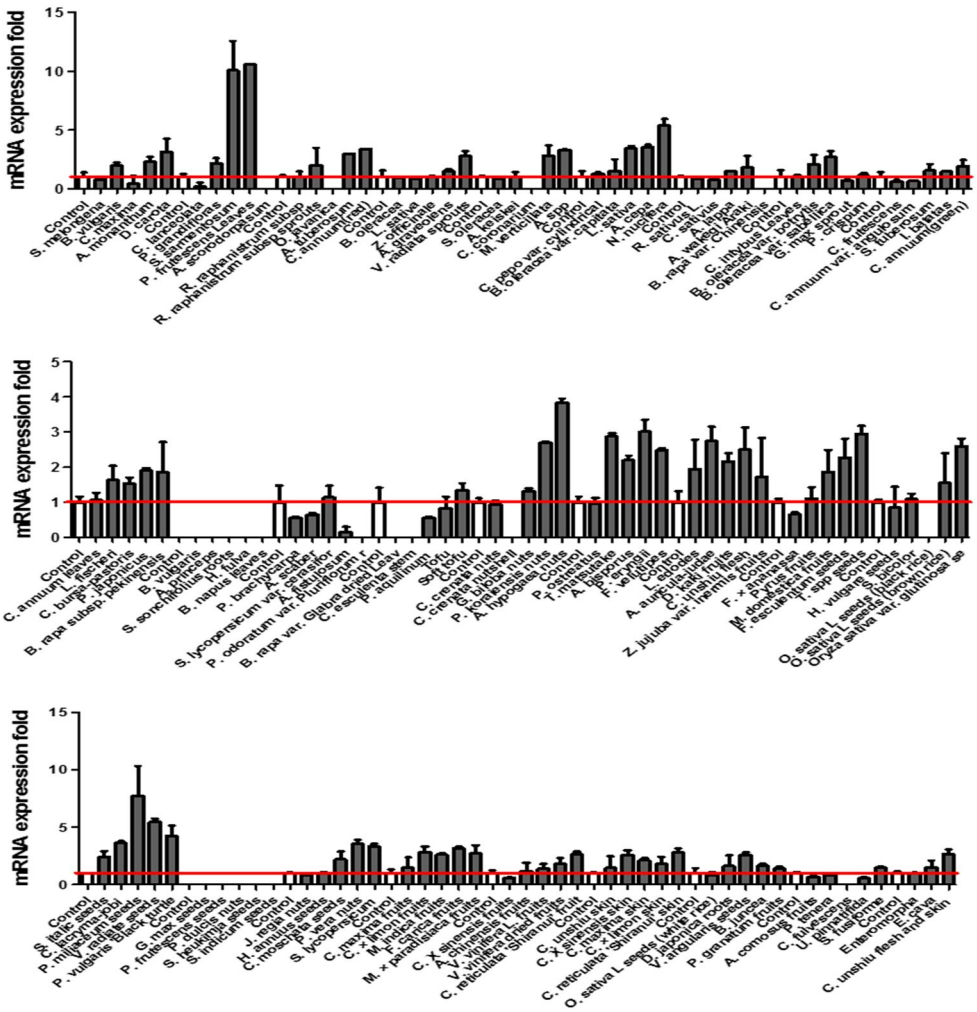

Figure 5. Screening of plant ethanolic extracts for activating IGF-1

mRNA expression.

HDFs were treated with diverse plant ethanolic extracts. After incubation for 6 h, cells were harvested and mRNA levels of IGF-1 were determined by RT-qPCR. All RT-qPCR experiments were performed two times. Each bar represents the mean ± SEM.

Figure. 6

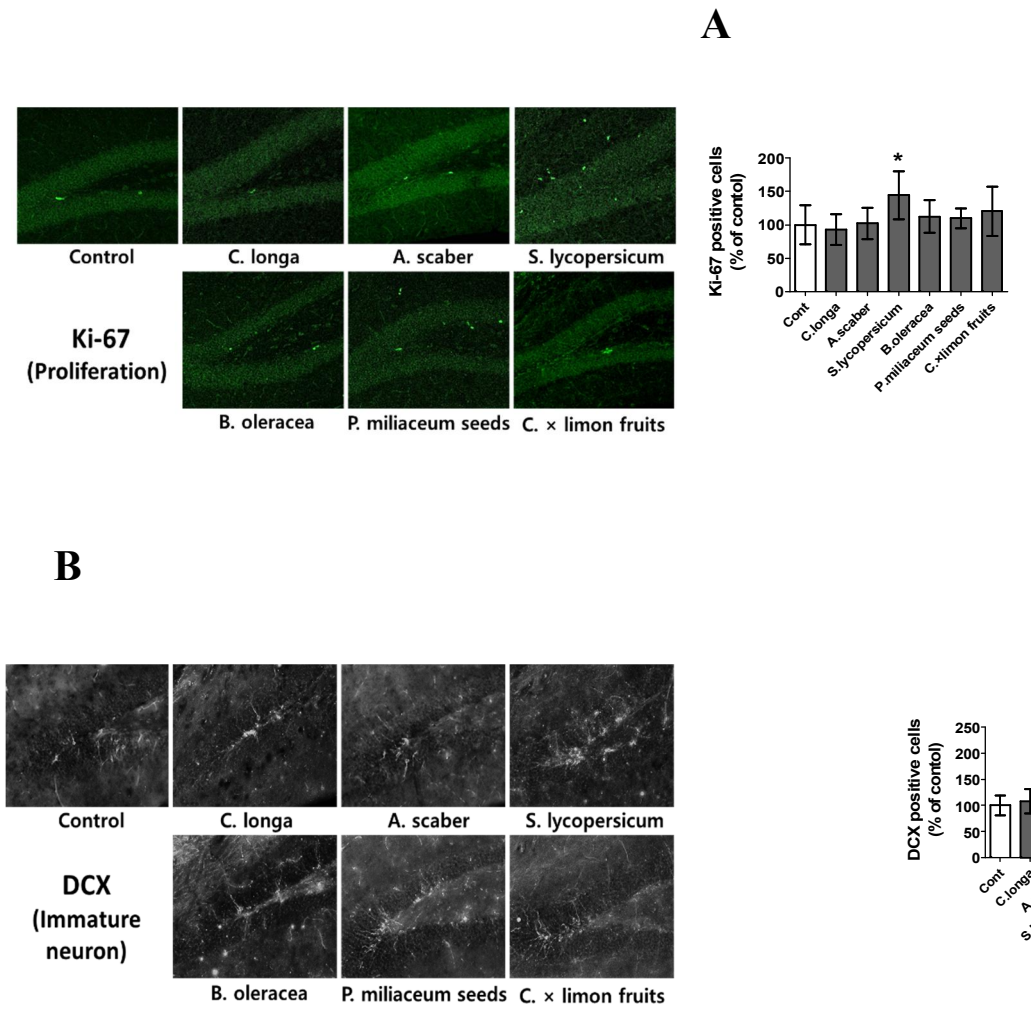

Figure 6. Effect of oral administration plant ethanolic extracts on hippocampal neurogenesis in aged mice.

To evaluate effects of plant ethanolic extracts on hippocampal neurogenesis in DG, ethanolic extracts of turmeric, aster scaber, tomato, broccoli, proso millet and lemon were orally administered to 18-month-old aged Skh-1 hairless mice once a day for 4 weeks. After biopsy brain sections were stained with antibodies against Ki-67 and DCX. (A) Representative photographs of Ki-67^{+} cells in hippocampal were shown. Total number of Ki-67^{+} cells in the DG were quantified in the graph in the right panel. (B) Representative photographs of DCX^{+} cells in hippocampal were shown. Total number of DCX^{+} cells in the DG were quantified in the graph in the right panel. Each bar represents mean±SEM of each group (n=6). Asterisks denote significant difference (*, $P < 0.05$; **, $P < 0.01$).

CHAPTER II

Effects of *Perilla frutescens* leaves extract on ultraviolet radiation-induced extracellular matrix damage in human dermal fibroblasts and hairless mice skin

INTRODUCTION

Perilla frutescens (L.) Britt. (Lamiaceae) is a widely-cultivated traditional medical herb that is commonly consumed in East Asian countries including Japan, China, and Korea. According to the theory of Korean traditional medicine, it is known that *P. frutescens* has long been used in Korea as a traditional medicine for skin irritation and allergy. Several recent reports described the effects of *P. frutescens* leaf extract (PLE) and its ingredients in skin diseases. 7,12-Dimethylbenz[a]anthracene (DMBA)- and 12-O-tetradecanoylphorbol-13-acetate (TPA)-induced skin tumors in mice were significantly inhibited by topical application of PLE and triterpene acids from *P. frutescens* leaves [22,23]. Oral administration of luteolin isolated from *P. frutescens* leaves produced anti-inflammatory and antipruritic effects in pruritogen-induced itching in mice [24]. Other physiological effects of *P. frutescens* in several diseases have also been reported in the literature.

Aromatic substances of *P. frutescens* seed oil are used to treat depression-related diseases and asthma as a traditional medicine [25,26]. Anti-inflammatory effects of *P. frutescens* leaves were demonstrated in cells stimulated using lipopolysaccharide- or N-formyl-Met-Leu-Phe [27,28] and in an inflammatory animal model [29].

Furthermore, oral administration of perilla extract decreased body weight and improved blood lipid profiles in high fat diet-fed mice [30].

Perilla seed oil is a rich source of unsaturated fatty acids and contains a very high level of n-3-alpha-linolenic acid (Asif, 2011). PLE also contains many active biological components including rosmarinic acid, luteolin, apigenin, ferulic acid, catechin, and caffeic acid (Peng et al., 2005). There has been increasing interest in the therapeutic prowess of *P. frutescens* and its pharmacological actions have been studied. But, the effect of PLE on skin aging is unclear.

This study investigated whether PLE can curb photo-aging in primary human dermal fibroblasts (HDFs) by analyzing the expression of MMP-1 and collagen, and the underlying signal pathway(s) involved. The *in vivo* efficacy of PLE was also assessed using UV-irradiated mice.

METERIALS AND METHODS

Materials and Cell culture

3-(4,5-dimethylthiazol-2-yl)-2,5-diphenyltetrazolium bromide (MTT) was purchased from Sigma (St. Louis, MO, USA). Antibodies against MMP-1 and type I procollagen (SP1.D8) were from Lab Frontier (Seoul, Korea) and Developmental Studies Hybridoma Bank (Iowa City, IA, USA), respectively. Specific antibodies for phospho-c-Jun and c-Jun were purchased from Cell Signaling (Beverly, MA, USA). Anti-actin (I-19) was obtained from Santa Cruz (Santa Cruz, CA, USA). HDFs were isolated from foreskin of young volunteers aged 10-19 years and cultured in Dulbecco's modified Eagle's media (DMEM; Gibco-BRL, Carlsbad, CA, USA), supplemented with 10% fetal bovine serum (FBS; Gibco-BRL) and penicillin/streptomycin (400 U/mL, 50 g/L) at 37°C in a humidified condition with 5% CO_2. This study was approved by the Institutional Review Board at Seoul National University Hospital (IRB.NO-1101-116-353), and all subjects provided written informed consent. The study was conducted in accordance with the Principles of the Declaration of Helsinki.

UV irradiation and PLE treatment

Philips TL 20W/12 RS fluorescent sun lamps with an emission spectrum between 275 and 380 nm (peak, 310–315 nm) were used as a UV source [31], and a Kodacel filter (TA401/407; Kodak, Rochester, NY) was used to block UVC (<290 nm). Irradiance was measured using a Waldmann UV meter (model 585100) [32]. After 24 h starvation, HDFs were washed with PBS and irradiated with UV. PLE powder dissolved in DMSO were treated into culture media.

MTT Assay

Cell viability was analyzed by using MTT assay. HDFs were seeded into 96-well plates and incubated with PLE (1, 5, 20, or 40 μg/ml) for 48h. After incubation, MTT solution (0.5 g/L in PBS) was treated for 4h. The culture media was removed and the formazan crystals dissolved in DMSO were quantified at 570 nm using ELISA reader (Thermo Fisher Scientific Inc., Waltham, MA, USA)

Western blot analysis

Western blot analysis was performed as described previously [20]. HDFs were lysed with 50 mM Tris-HCl (pH 7.4) buffer with protease inhibitor and phosphatase inhibitor cocktails (Sigma-Aldrich, St. Louis, MO). Protein quantities of cell lysates were determined using BCA reagent (Sigma-Aldrich). Equal amounts of protein was separated by

SDS-polyacrylamide gel electrophoresis, and then transferred to PVDF membrane (Amersham, Buckinghamshire, UK). The membrane was blocked in 5% skim milk in TBST and incubated with primary antibodies. The blots were further incubated with horseradish peroxidase-conjugated secondary antibody. Blotting protein were visualized using an ECL detection system (GE Healthcare, UK).

Reverse transcription and real-time quantitative PCR

Total RNA was isolated from HDFs using RNAiso Plus (Takara Bio Inc., Shiga, Japan) as previously described [21]. cDNAs were synthesized from isolated RNA templates using a First Strand cDNA Synthesis Kit (MBI Fermentas, Vilnius, Lithuania). The cDNAs were subject to quantitative PCR. PCR products was quantitated by 7500 Real time PCR System (Applied Biosystems, Foster City, CA, USA) with SYBR Premix Ex Taq II kit (Takara Bio). The PCR reactions were performed with the following primers; Type I procollagen, MMP-1 and endogenous reference 36B4. Data were analyzed using the $2^{-\Delta\Delta CT}$ methods and expressed as fold changes of gene expression relative to 36B4.

AP-1 DNA binding assay

HDFs were suspended in cytoplasmic extraction buffer (20 mM Tris,

1.5 mM $MgCl_2$, 10 mM KCl, 0.2 mM EDTA, 0.5 mM dithiothreitol, 0.5% Nonidet P-40, and protease inhibitor cocktail) and incubated in ice for 10 min followed by centrifugation at 6,000 rpm for 5 min at 4°C to separate the nuclear pellet. The pellet was re-suspended with vortexing in nuclear extraction buffer (cytoplasmic extraction buffer with 400 mM NaCl and 5% glycerol) and incubated in ice for 30 min. The pellet was centrifuged at 12,000 rpm for 10 min at 4°C to obtain the nuclear fraction. An electrophoretic mobility shift assay (EMSA) was performed using an AP-1 EMSA kit according to the manufacturer's instructions (Affymetrix, Santa Clara, CA, USA). Briefly, biotin-labeled AP-1-specific probes were incubated with 10 mg of nuclear extract. Binding reactions were performed at 15°C for 30 min to allow the formation of transcription factor/DNA complexes. The complexes were separated by 6% non-denaturing PAGE in 0.5X TBE and transferred onto a Hybond-N nylon membrane (Amersham). The labeled complex was visualized using an ECL imaging system.

Detection of ROS production

HDFs were pretreated with N-acetylcysteine (NAC) or PLE for 4h in serum-free media and then washed with PBS. After washing the cells, 20 mM of 2',7'-dichlorofluorescin diacetate (DCF-DA) in Hank's Balanced Salt Solution (HBSS) was treated and incubated at 37℃ for

30 min. 100 mJ/cm^2 of UV was treated to induce ROS generation. The cells were washed twice with PBS and warm HBSS was added. Cells were then assayed using the Victor3 multilabel plate reader (PerkinElmer, Waltham, MA, USA) at an excitation wavelength of 485 nm and an emission wavelength of 535 nm.

Liquid Chromatography (LC) mass spectrometry (MS)/MS analysis

PLE was analyzed using an Ultra Performance Liquid Chromatography (UPLC) system (Waters, Milford, MA, USA) equipped with an Acquity UPLC BEH C_{18} column (100×2.1 mm, 1.7 μm; Waters) that was equilibrated with water containing 0.1% formic acid. The sample was eluted in a gradient with acetonitrile containing 0.1% formic acid at a flow rate of 0.35 mL/min for 10 min. The eluted compounds were analyzed by a Quadrupole Time-of-Flight (Q-TOF) mass spectrometer (Waters) in electrospray ionization-positive mode. The voltages of the capillary and sampling cones were set at 3 kV and 30 V, respectively. The temperatures of the source and desolvation were set at 110°C and 350°C, respectively, and the desolvation flow rate was 800 L/h. TOF MS data were collected in the *m/z* 100–1200 range with a scan time of 0.1 s. Lock spray with leucine-enkephalin (556.2771 Da) was used at a flow rate of 20 μL/min and a frequency of 10 s to ensure

accuracy and reproducibility for all analyses. The MS/MS spectra of the metabolites were collected in the *m/z* 70–1200 by a collision energy ramp from 20–45 eV. All MS data obtained by MassLynx software (Waters), including retention time, *m/z*, and ion intensity were analyzed using MarkerLynx software (Waters). The compounds were identified using human metabolome databases (www.hmdb.ca), the METLIN database (metlin.scripps.edu), and previous literature data [33,34].

Animals and treatments

Seven-week-old female albino hairless (Skh-1) mice were obtained from Orient Bio Inc. (Seoul, Korea). The mice were acclimated for 1 week prior to the study and had free access to food and water. All experimental protocols were approved by the Institutional Animal Care and Use Committees (IACUC No. 14-008-S1A0) at Seoul National University. UV treatment was performed as described previously [35]. Minimal erythema dose (MED) was measured on the dorsal skin of mice. Mice were divided into four groups: (i) sham-irradiated vehicle-treated mice, (ii) sham-irradiated, PLE (0.5%)-treated mice, (iii), UV-irradiated and vehicle-treated mice, and (iv) UV-irradiated and PLE (0.5%)-treated mice. The vehicle was composed of ethanol/polyethylene glycol (3:7, v/v). Vehicle and PLE were topically applied to the dorsal skin after UV irradiation. These mice were

sacrificed at 48 h post-UV and skin specimens were obtained.

Hematoxylin and eosin (H&E) staining and skin thickness measurements

Skin samples were fixed with 4% paraformaldehyde in PBS overnight at 4°C and embedded in paraffin. Four micrometer-thick paraffin sections were mounted on silane-coated slides and stained with H&E. Images were taken with a model D70 microscopic digital camera (Olympus, Tokyo, Japan) connected to a BX51 light microscope (Olympus). Epidermal thickness was measured using Image J analysis software (NIH, Bethesda, MD, USA).

Statistical analysis

All data were analyzed using SPSS software (IBM, Armonk, NY, USA). Results are expressed as mean±SEM. Student's t test and Mann-Whitney test was used for the in vitro and in vivo statistical analysis, respectively. *P*-values < 0.05 were considered statistically significant.

RESULTS

PLE inhibited both basal and UV-induced MMP-1 and MMP-3 expression

To investigate whether PLE affected the expression of collagenase expression, HDFs were treated with various concentrations of PLE after UV or sham irradiation. After incubation for 48 h, culture medium was harvested to determine expression levels of MMP-1 and MMP-3 using Western bloting. PLE suppressed the basal expression of MMP-1 and MMP-3 (**Figure 7A**) and decreased UV-induced MMP-1 expression in a dose-dependent manner (**Fig. 1B**). Consistently, both basal (**Figure 7C**) and UV-induced (**Figure 7D**) MMP-1 and MMP-3 mRNA were significantly suppressed by PLE in a dose-dependent manner. These results indicate PLE inhibition of MMP-1 and MMP-3 production.

PLE inhibited UV-induced mitogen-activated protein kinase (MAPK) signaling pathways

MAPK signaling pathways including ERK, JNK, and p-38 regulate UV-induced MMP-1 and MMP-3 expression by activating AP-1 [36]. To determine an appropriate UV exposure time to activate MAPK

signaling pathways, HDFs treated with UV were harvested at pre-determined times. UV significantly increased ERK, JNK, and p-38 phosphorylation within 15 min post-UV, which subsequently returned to the basal levels (**Figure 8A**). To investigate whether the MAPK signaling pathways were involved in reduction of UV-induced MMP-1 and MMP-3 expression by PLE, HDFs were treated with PLE for 2 h after UV irradiation, and the levels of ERK, JNK, and p-38 phosphorylation were evaluated by Western bloting at 15 min post-UV. Treatment with PLE inhibited phosphorylation of ERK, JNK, and p-38 in a dose-dependent manner (**Figure 8B**). These results suggest that inhibition of MAPK signaling pathways by PLE might prevent UV-induced MMP-1 and MMP-3 expression.

Treatment of PLE suppressed UV-induced AP-1 activation

The MMP-1 promoter includes a binding site for AP-1. AP-1 is critical in UV-induced MMP-1 expression [37]. To investigate the effects of PLE in UV-induced AP-1 activities, cells were treated with PLE for 4 h after UV irradiation. DNA binding activity of AP-1 was inhibited dose-dependently after treatment of PLE (**Figure 9A**). Since AP-1 is composed of the Jun and Fos families, I investigated the effects of PLE on c-Jun phosphorylation and c-Fos expression in nuclear extracts of UV-irradiated HDFs. Phosphorylated forms of c-Jun in

nuclear extracts were decreased by PLE in a dose-dependent manner. In addition, UV-induced expression of c-Fos in nuclear extracts was reduced by PLE (**Figure 9B**).

PLE suppressed UV-induced ROS generation

Next I investigated whether PLE inhibits UV-induced MMP-1 expression through an antioxidant effect. UV irradiation significantly increased ROS production by 250±28% versus the control. However, PLE pretreatment reduced UV-induced ROS generation to a level similar to the positive control, N-acetylcysteine (**Figure 10A**). To identify bioactive molecules with antioxidative effects in PLE, UPLC-Q-TOF MS was performed. Although two major compounds (m/z 593 → 533 and m/z 621 → 561) were not identified, the antioxidant luteolin-diglucuronide, apigenin-diglucuronide, luteolin-glucuronide, and rosmarinate were identified as major compounds of PLE (**Figure 10B**). This result demonstrated that the inhibitory effects of PLE in UV-induced MMP-1 expression might be attributed to antioxidant effects by several antioxidant molecules.

PLE increased Type I procollagen production

To investigate the effect of PLE on type I procollagen production, HDFs were treated with various concentrations of PLE for 48 h after

UV or sham irradiation. The supernatant from HDFs was analyzed for protein expression of type I procollagen. PLE significantly increased the basal expression of type I procollagen in a dose-dependent manner (**Figure 11A**). In addition, UV-reduced type I procollagen expression was significantly increased by PLE treatment compared to non-treated control (**Figure 11B**). To investigate whether cell proliferation can affect type I procollagen production, HDF viability was analyzed using the MTT assay. PLE did not affect cell proliferation irrespective of UV irradiation (**Figure 11C and D**). These results suggest that PLE has the potential to increase type I procollagen production.

PLE inhibited UV-induced epidermal skin thickening

To investigate the effects of PLE on UV-exposed skin in hairless mice, 0.5% PLE was topically applied on hairless mice after UV irradiation. Histological changes of skin were shown in **Figure 12A**. UV irradiation significantly increased epidermal thickness by 90.0±22.1% versus the control. However, UV-induced epidermal thickening was significantly inhibited by 0.5% PLE. On the other hand, sham-irradiated PLE-treated group showed no significant changes in epidermal thickness (**Figure 12B**). The relative difference of skin thickening was reduced in the PLE-treated group with UV irradiation, compared with PLE-treated group without UV irradiation (**Figure 12C**)

PLE inhibited UV-induced MMP-13 expression

To investigate the effects of PLE on MMP-1 and type I collagen expression in hairless mice, I analyzed MMP-13 expression in mouse skin tissues, since MMP-13 is a functional substitute for MMP-1 in mice skin. UV irradiation significantly increased MMP-13 protein expressions by 181.4±44.0 %, while this induction was significantly inhibited by 47.9±16.7 % in PLE-treated group compared with UV-treated group (**Figure 13A**). On the other hand, PLE did not prevent UV-induced decrease of type I collagen compared with UV-treated group (**Figure 13B**). Type I collagen expression in sham-irradiated PLE-treated group increased by 34.4±8.1 % compared with vehicle-treated group, albeit not significant.

Figure. 7.

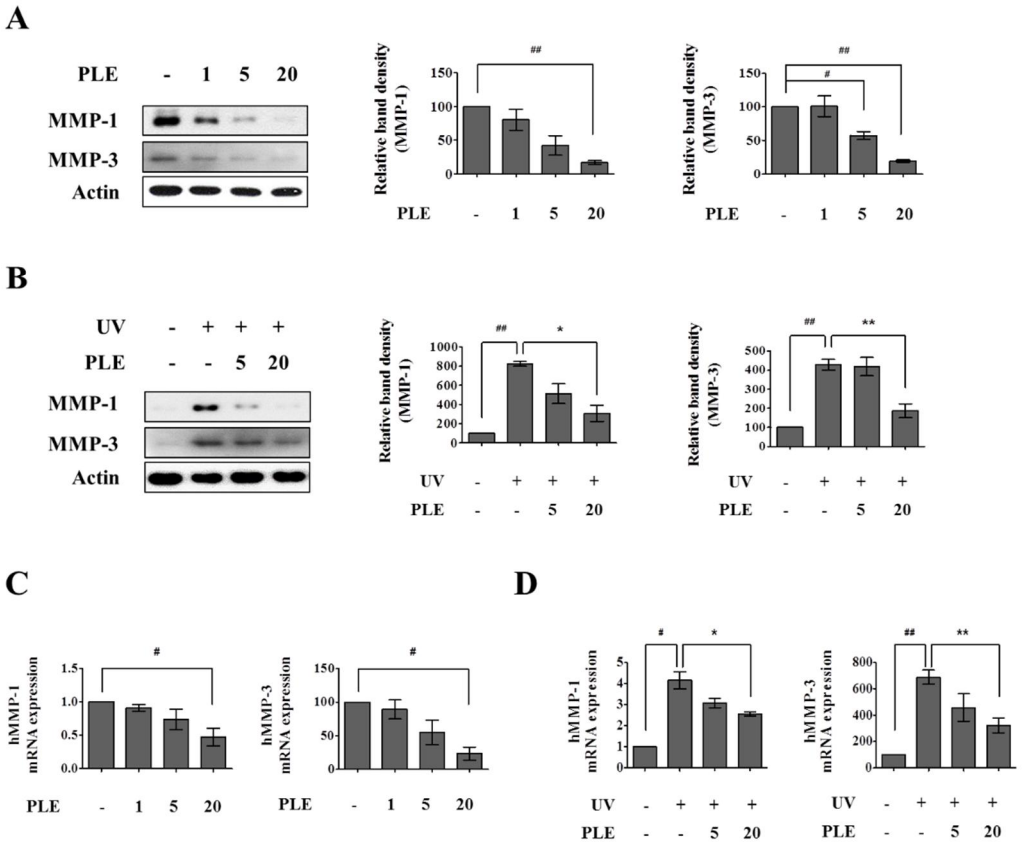
A
PLE - 1 5 20
MMP-1
MMP-3
Actin
Relative band density (MMP-1)
Relative band density (MMP-3)
B
UV - + + +
PLE - - 5 20
C
hMMP-1 mRNA expression
hMMP-3 mRNA expression
D

Figure 7. PLE reduced basal and UV-induced MMP-1 and MMP-3 expression in HDFs.

(A) Cells were treated for 48 h with PLE at concentrations of 1, 5, or 20 μg/ml. Culture medium was harvested and MMP-1 and MMP-3 expression was measured by western blotting. (B) Cells were irradiated with 100 mJ/cm^2 of UV and treated with PLE for 48 h. Culture medium was harvested and MMP-1 and MMP-3 expressions were measured by Western blotting. Relative protein expressions were analyzed using Image J analysis software. Intensity of MMP-1 and MMP-3 were normalized to that of corresponding actin. The mRNA levels of MMP-1 and MMP-3 with (C) sham or (D) UV irradiation were determined by quantitative RT-PCR at 48 h after PLE treatment. MMP-1 mRNA expression was normalized to 36B4. Each bar represents the mean±SEM of three independent experiments. #P<0.05, ##P< 0.01 versus sham-irradiated group, *P<0.05 versus UV-irradiated group

Figure. 8.

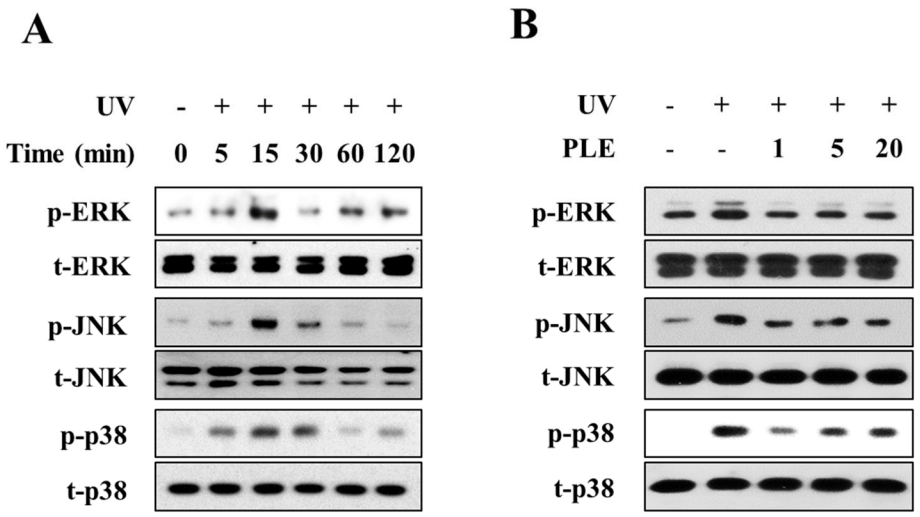

Figure 8. PLE inhibited UV-induced MAPK signaling pathways in HDFs. (A) HDFs were irradiated with 100 mJ/cm^2 of UV and harvested at indicated times. Changes in phosphorylated form of ERK, JNK and p-38 were analyzed by western blotting using phospho-specific ERK, JNK and p-38 antibodies. (B) Cell were irradiated with 100 mJ/cm^2 of UV and treated with PLE at concentrations of 1, 5, or 20 μg/ml. Levels of ERK, JNK, and p-38 phosphorylation at 15 min after UV treatment were examined by Western blotting. Total ERK, JNK, and p-38 protein was used as a loading control.

Figure. 9

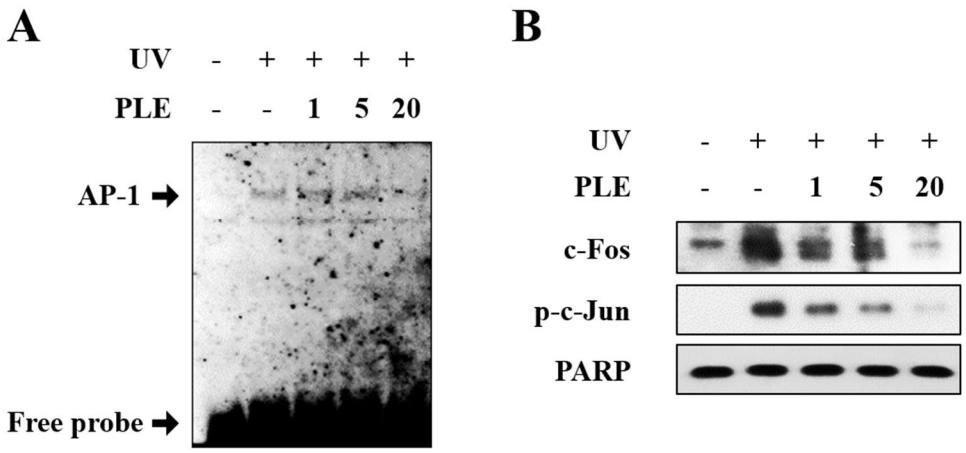

Figure 9. PLE suppressed UV-induced AP-1 activation in HDFs.

(A) Cells were irradiated with 100 mJ/cm^2 of UV and treated with PLE (1, 5, or 20 μg/ml) for 4 h. After UV treatment, nuclear fractions were extracted and incubated with biotin-labeled AP-1 oligonucleotides for non-radioactive EMSA. Arrows indicate the AP-1 complex and free AP-1 oligonucleotide. (B) Nuclear extracts were examined by western blotting using c-Fos and phospho-specific c-Jun antibodies. The poly ADP ribose polymerase band was used as a loading control for nuclear extracts.

Figure. 10.

A

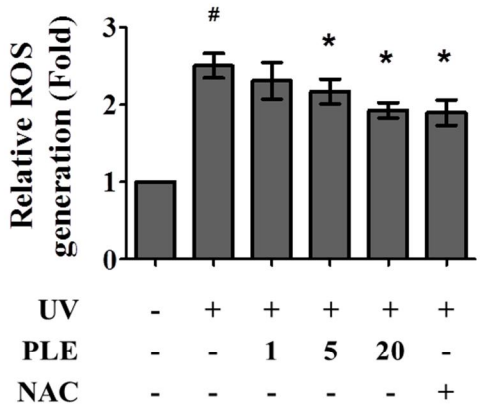
Relative ROS generation (Fold)
0
1
2
3
#
*
*
*
UV - + + + + +
PLE - - 1 5 20 -
NAC - - - - - +

B

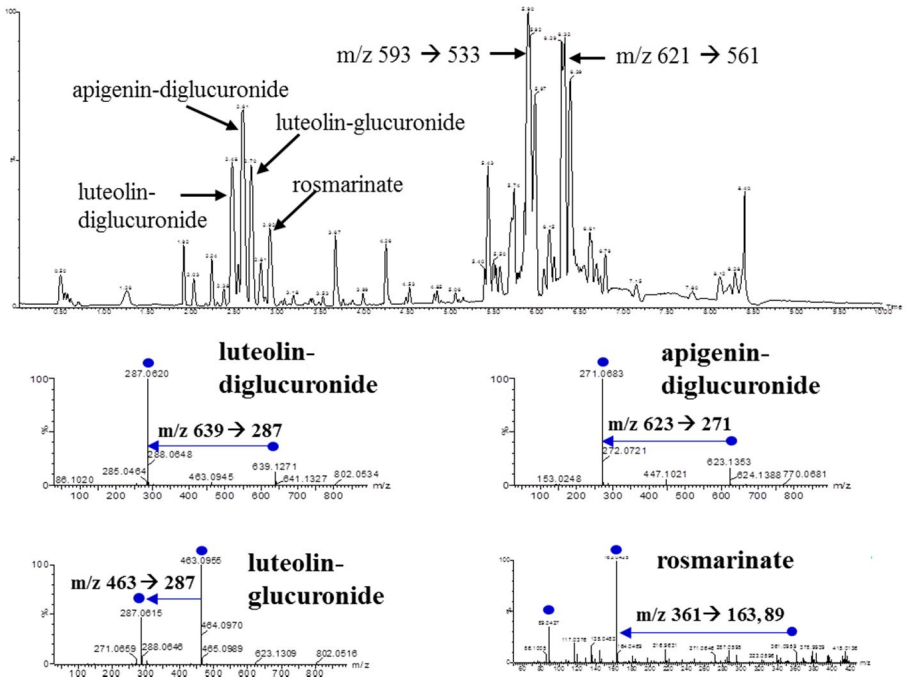
m/z 593 → 533
m/z 621 → 561
apigenin-diglucuronide
luteolin-glucuronide
luteolin-diglucuronide
rosmarinate
luteolin-diglucuronide
m/z 639 → 287
apigenin-diglucuronide
m/z 623 → 271
luteolin-glucuronide
m/z 463 → 287
rosmarinate
m/z 361→ 163, 89

Figure 10. PLE suppressed ROS generation in HDFs.

(A) Cells were pretreated with PLE at indicated concentrations or N-acetylcysteine (NAC, 10 ng/ml) for 4 h followed by 100 mJ/cm^2 of UV irradiation. Cells were washed with HBSS and treated with 20 μM of 2',7' –dichlorofluorescin diacetate. After a 30-min incubation, cells were analyzed using a fluorescence reader. (B) A base peak ion chromatogram of PLE analyzed using UPLC-Q-TOF-MS and mass spectra of four major compounds (luteolin-diglucuronide, apigenin-diglucuronide, luteolin-glucuronide, and rosmarinate). Each bar represents mean±SEM of three independent experiments. #P<0.05 versus sham-irradiated group, *P<0.05 versus UV-irradiated group

Figure. 11.

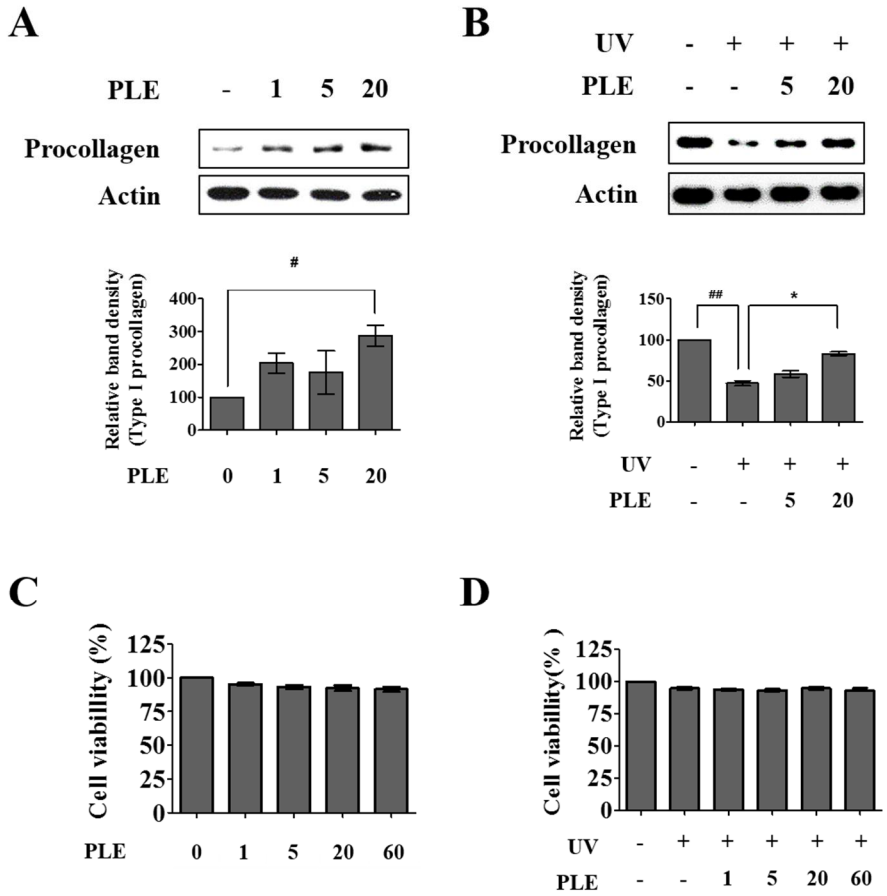
A
PLE - 1 5 20
Procollagen
Actin
Relative band density (Type I procollagen)
400
300
200
100
0
#
PLE 0 1 5 20
B
UV - + + +
PLE - - 5 20
Procollagen
Actin
Relative band density (Type I procollagen)
150
100
50
0
##
*
UV - + + +
PLE - - 5 20
C
Cell viabillity (%)
125
100
75
50
25
0
PLE 0 1 5 20 60
D
Cell viabillity(%)
125
100
75
50
25
0
UV - + + + + +
PLE - - 1 5 20 60

Figure 11. PLE promotes type I procollagen expression in HDFs.

(A) HDFs were treated with PLE (1, 5, or 20 μg/ml) for 48 h. Culture medium was harvested and type I procollagen expression was measured by Western blotting. (B) Cells were irradiated with 100 mJ/cm^2 of UV and treated with PLE for 48 h. Culture medium was harvested and type I procollagen expression was measured by Western blotting. Relative protein expressions of type I procollagen were analyzed using Image J analysis software. Intensity of type I procollagen was normalized to that of actin. Cells were treated with PLE (1, 5, 20, or 60 μg/ml) for 48 h after (C) sham- or (D) UV radiation (100 mJ/cm^2). Cell viability was analyzed by MTT assay. Each bar represents mean±SEM of three independent experiments. #P< 0.05, ##P< 0.01 versus sham-irradiated group, *P < 0.05 versus UV-irradiated group

Figure. 12.

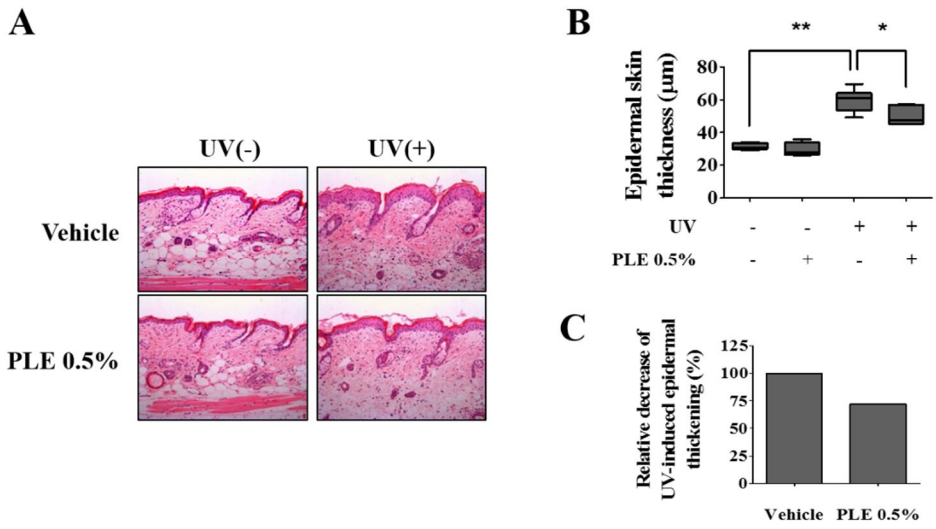

Figure 12. PLE inhibited UV-induced epidermal skin thickening in hairless mice.

0.5% PLE were topically applied to UV-irradiated and non-irradiated dorsal skin of mice. After overnight fixation with 4% paraformaldehyde, 4 μm of paraffin sections was stained with hematoxylin and eosin (H&E). (A) The photographs are representative H&E-stained skin (×200). (B) Epidermal skin thicknesses are analyzed using H&E-stained sections. (C) The relative difference of epidermal thickness between UV- and non-irradiated mice groups are analyzed. Results are analyzed using ImageJ analysis software and represents

mean±SEM of each group (n=6). Asterisks in all graphs denote statistically significant difference (*, $P<0.05$; **, $P<0.01$).

Figure. 13.

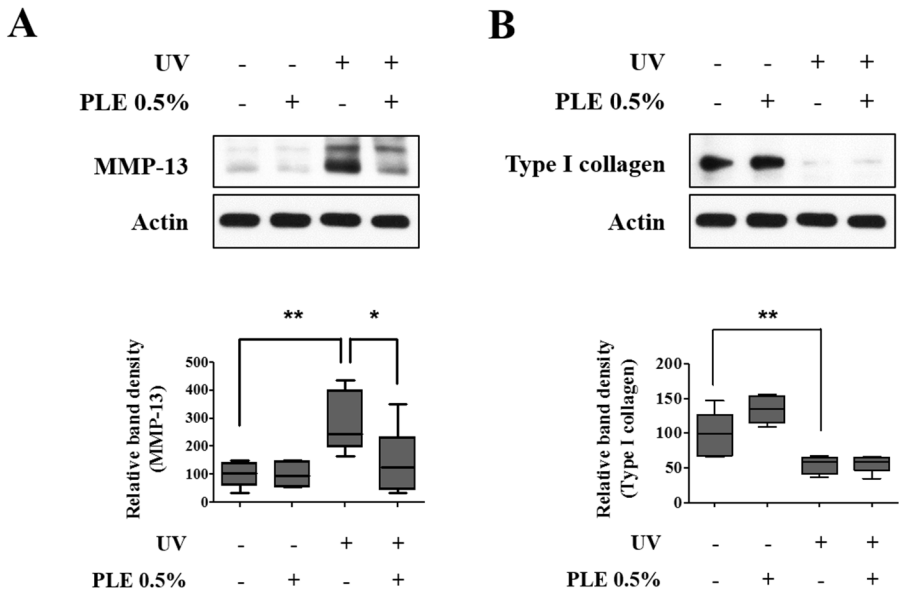

Figure 13. PLE suppressed UV-induced MMP-13 expression and promotes type I collagen expression.

0.5% PLE were topically applied to UV-irradiated and non-irradiated dorsal skin of mice. At 48 h after UV irradiation, skin samples were obtained, lysed and subjected to western blotting using MMP-13 and type I collagen antibodies. The bands shown are representative of each group. Relative protein expressions of MMP-1 (A) and type I collagen (B) were analyzed using ImageJ software. Intensity of bands are normalized to actin. Each bar represents the mean±SEM of each group (n=6). Asterisks in all graphs denote statistically significant difference (*, $P<0.05$; **, $P<0.01$).

CHAPTER III

Effects of *Lycopersicon esculentum* extract on cognitive function and hippocampal neurogenesis in aged mice

INTRODUCTION

Tomato (*Lycopersicon esculentum*) is consumed worldwide as a raw fruit or in processed products, and it is an important dietary source of nutrients such as polyphenols, flavonoids and several antioxidants. Diverse active compounds in tomato have shown pharmacological efficacy in several types of cancer [38], endothelial function [39], obesity [40] and neuroprotection [41]. Recent reports have demonstrated that tomato seed extract reduced oxidative stress and neurotoxicity in a rotenone-induced Parkinson's disease (PD)-like mouse model [42]. Lycopene (a major antioxidant in tomato) also has a neuroprotective effect on 1-methyl-4-phenyl-1,2,3,6-tetrahydropyridine (MPTP) -induced PD in mice through improvement of mitochondrial impairment and inflammation [43]. However, the neurogenic and cognitive-enhancing effects of tomato in aged mice has not yet been elucidated.

To investigate the effects of tomato on the cognitive function, extracts of tomato were prepared using 50% ethanol extraction method, and the extracts were orally administered to 12-month-old aged mice once a day for 6 weeks. Novel object recognition (NOR) test and BDNF signaling pathway in the hippocampus were evaluated for the efficacy of TEE in this study.

METERIALS AND METHODS

Antibodies

The antibodies used in this study were as follows; mouse monoclonal antibodies against postsynaptic density-95 (PSD-95) (ab2723, Abcam, Cambridge, UK), goat polyclonal antibodies against β-actin (sc-1616, Santa Cruz Biotechnology, Santa Cruz, CA, USA), goat polyclonal antibodies against doublecortin (DCX) (sc-8066, Santa Cruz Biotechnology), rabbit polyclonal antibodies against phospho-ERK (#9101S, Cell Signaling Technology, Danvers, MA, USA) and polyclonal antibodies against total ERK (#9102, Cell Signaling Technology)

Preparation of the tomato ethanolic extract (TEE).

TEE was prepared by Korea Food Research Institute (Seongnam-si, Korea). Tomatoes were sliced, shade dried, powdered, and sequentially extracted with 50 % alcohol twice, 3 h each. The extract was filtered, then condensed by vacuum and freeze-dried at -40 °C under reduced pressure (yield: 46.18% of dry weight).

Animals and TEE administration

Twelve-month-old aged and 8-week-old young female albino hairless mice (Skh-1) were purchased from Orient Bio (Seongnam-si, Korea). Animals were allowed to feed *ad libitum*, and acclimated for 1 week prior to the study. All experimental protocols were approved by the Institutional Animal Care and Use Committee of Center for Phenogenomics Animal Research Facility, Woojung BSC (Suwon, Korea, Association for Assessment and Accreditation of Laboratory Animal Care-accredited facility). The aged mice were randomly divided into two equivalent groups: those with vehicle or TEE administration. The animals were orally fed with a dose of 400 mg/kg using a feeding needle once daily for 6 weeks and were sacrificed 6 h after the last administration. For vehicle-treated young and aged mice, the same volume (i.e. 0.2 ml) of 0.5% carboxymethyl cellulose-sodium solution was administered once daily for 6 weeks (**Figure 14A**). Each group composed of nine mice and vehicle-treated young mice were used as positive control.

Novel object recognition test (NOR)

To evaluate cognitive function of mice, NOR test, a non-forced recognition memory test, was performed using a modified method [44]. Briefly, the apparatus consists of an opaque plastic chamber (25 cm×25 cm). The procedure includes 3 phases: habituation, training and testing.

On the first day, mice were allowed to freely explore the chamber without objects for 5 min to familiarize with the environment (habituation phase). On the second day, mice were given 5 min of exposure using the identical pair of objects (training phase). For short-term memory retention, mice were placed in the chamber 1 h later with one of the previous objects and a novel object for 5 min (testing phase) (**Figure 14B**). Both training and testing sessions were recorded with a video camera and analyzed by investigators blinded to the group allocation.

Sample collection

The mice were anesthetized with an intramuscular injection of Zoletil (Virbac, Fort Worth, TX, USA) and xylazine solution (3:1 ratio), and transcardially perfused with 0.9% normal saline. Brains were carefully dissected, and separated into two hemispheres. For biochemical analyses, hippocampus was removed from the left hemisphere and snap-frozen in liquid nitrogen, and stored at −80 °C. The right hemisphere was fixed with 4% paraformaldehyde in PBS for overnight at 4°C and equilibrated in 30% sucrose. The brain tissues were cut into sequential coronal sections (40 μm thick) with a cryostat (Leica, Nussloch, Germany) and collected individually in 24-multiwell culture plates.

Doublecortin immunohistochemistry

Immunostaining for DCX was performed using the free floating technique. One series was randomly selected, and stained using antibodies against DCX (Santa Cruz Biotechnology). The free floating slices were incubated for 2 days at 4°C with the primary antibodies in a diluent buffer (1% bovine serum albumin (BSA) and 1% Triton X-100 in 0.1 M phosphate buffer). Subsequently, sections were incubated for 24h at 4°C with biotinylated rabbit anti-goat IgG antibody (Vector Laboratories Ltd, Burlingame, CA, USA). The sections were then incubated with Vector ABC kit. DCX-positive cells were visualized with 3,3′-diaminobenzidine (DAB). The images were taken with a Leica DM5500B microscope (Leica). To quantify the total number of DCX-positive cells in the SGZ, all sections were coded and cell counting was performed with the examiner blinded to group allocation.

Enzyme-linked immunosorbent assay (ELISA)

Hippocampus was homogenized in lysis buffer (20 mM Tris, 137 mM NaCl, 1% NP-40 detergent, 10% glycerol, 1 mM phenylmethylsulfonylflouride (PMSF), 10 μg/mL aprotinin, 1 μg/mL leupeptin, and 0.5 mM sodium orthovanadate; pH 7.2) and then centrifuged at 14,000 rpm for 15 min at 4°C. The supernatants were

used for analysis. To measure endogenous corticosterone and BDNF levels in hippocampus, ELISA was performed using the Corticosterone ELISA kit (Enzo Life Sciences, NY, USA) and the BDNF Emax Immunoassay System (Promega, Madison, WI, USA), respectively. All procedures were carried out according to the manufacturer's instructions. Corticosterone and BDNF levels were quantified at 450 nm using ELISA reader (Thermo Fisher Scientific Inc., Waltham, MA, USA) and analyzed by a standard curve.

Western blot analysis

Western blot analysis was performed as previously described [45]. Protein quantity was determined using BCA reagent (Sigma-Aldrich, St. Louis, MO, USA). 20 μg of protein extract were separated by SDS-polyacrylamide gel electrophoresis, and then transferred to PVDF membrane (Amersham, Buckinghamshire, UK). The membrane was blocked in 5% fat-free milk in TBST (20 mM Tris-HCl, pH 7.6, containing 0.4% Tween 20) and incubated with primary antibodies for 24 h. The membrane were further incubated for 1h with horseradish peroxidase-conjugated secondary antibody. Proteins were visualized using an ECL detection system (GE Healthcare, UK).

Statistical analyses

The behavioral data were analyzed using unpaired Student's t-tests, and a p-value of less than 0.05 was considered to be statistically significant. The data from the immunohistochemistry, western blot and ELISA were analyzed using a one-way ANOVA with Newman-Kuels post hoc tests for the multiple comparisons tests. The results are expressed as means ± SEM, and the statistical analyses were performed using the SPSS 22.0 software (IBM, Armonk, NY, USA).

RESULTS

Oral TEE supplement did not affect body weight in aged mice

A total of eighteen mice (nine mice/group) completed the study. To examine whether TEE administration was associated with a change in the body weight of mice, the body weight was measured every week. Six weeks of TEE treatment did not influence the body weight of the mice when compared to the vehicle-treated group (**Figure 14C**).

Oral TEE supplement improved age-related memory impairment

During the training phase, there were no statistical differences in the percentage of time spent exploring two identical objects (**Figure 15A**). During the test phase, the vehicle-treated mice also showed a comparable percentage of time spent exploring the novel object (51.4±8.2%). However, the group with oral administration of TEE exhibited a significant increase in the percentage of time spent exploring the novel object (70.8±4.1%) as compared to familiar object (29.2±4.1%) (**Figure 15B**). As shown in **Figure 15C**, the discrimination index in the TEE-treated mice (0.4±0.1) was significantly higher than that of the vehicle-treated mice (0.0±0.2). Thus, the TEE administration could improve cognitive function in aged

mice, suggesting that TEE might have a cognition-enhancing effect against age-related memory decline.

Oral TEE supplement increased DCX+ cells and PSD95 protein expression in aged mice

The above results indicated that the TEE treatment enhanced cognitive function in aged mice. To investigate whether the TEE treatment affected hippocampal neurogenesis, the overall cell proliferation in the SGZ of the DG was assessed via immunohistochemistry for DCX, a marker for immature neurons. A significant reduction by 14.8-fold in the number of DCX+ cells in the DG in aged mice (12-month old) compared to young (8-week old) mice (720.0±101.2 vs. 10667.5±157.9; aged vs. young) was observed. However, the mice supplemented with TEE showed a significant increase (1.6-fold) in the number of DCX+ cells in DG (720.0±101.2 vs. 1132.0±117.9; vehicle vs. TEE) (**Figure 16A**). In addition, the PSD95 protein levels in the hippocampus were investigated for evaluating the changes of synapse formation and synaptic plasticity. The age-related reduction of PSD95 expression in aged mice was significantly up-regulated in the TEE-supplemented group (**Figure 16B**). These findings suggest that the cognition-enhancing effect of TEE is a result of the induction of hippocampal neurogenesis and synaptic plasticity in aged

mice.

Oral TEE supplement decreased corticosterone and increased BDNF in hippocampus

To investigate the possible mechanisms of cognition enhancement and neurogenesis for TEE, the corticosterone and BDNF levels in hippocampus were analyzed via ELISA. Although BDNF is significantly decreased in the hippocampus of aged mice when compared to young mice, TEE administration significantly increased the hippocampal BDNF protein by 32.6±6.7% in aged mice (**Figure 17A**). There was no statistical difference in the hippocampal corticosterone levels between young and aged mice. However, the levels of corticosterone in the TEE-treated mice hippocampus decreased significantly by 13.3±3.5% relative to vehicle-treated aged mice (**Figure 17B**).

Oral TEE supplement activated ERK/CREB signaling pathway

Chronic exposure to corticosterone down-regulates the BDNF expression, and decreases neurogenesis in the hippocampus [46]. In addition, the activation of the ERK/CREB signaling pathway induced by BDNF plays a critical role in hippocampal neurogenesis and cognition improvement [47]. To examine whether the TEE supplement

led to the activation of ERK and CREB in the hippocampus, the changes in the phosphorylation of ERK and CREB were investigated via Western blot analysis and immunohistochemistry, respectively. TEE administration significantly increased the levels of ERK phosphorylation in the hippocampus by 262.5% relative to vehicle-treated aged mice (**Figure 18A**). Furthermore, the TEE treatment significantly induced the phosphorylation of CREB in the SGZ of DG (**Figure 18B**). These results indicate that the TEE supplement can improve the age-dependent decrease in the hippocampal neurogenesis and cognition by activating the ERK/CREB pathway as well as increasing the BDNF production.

Figure. 14.

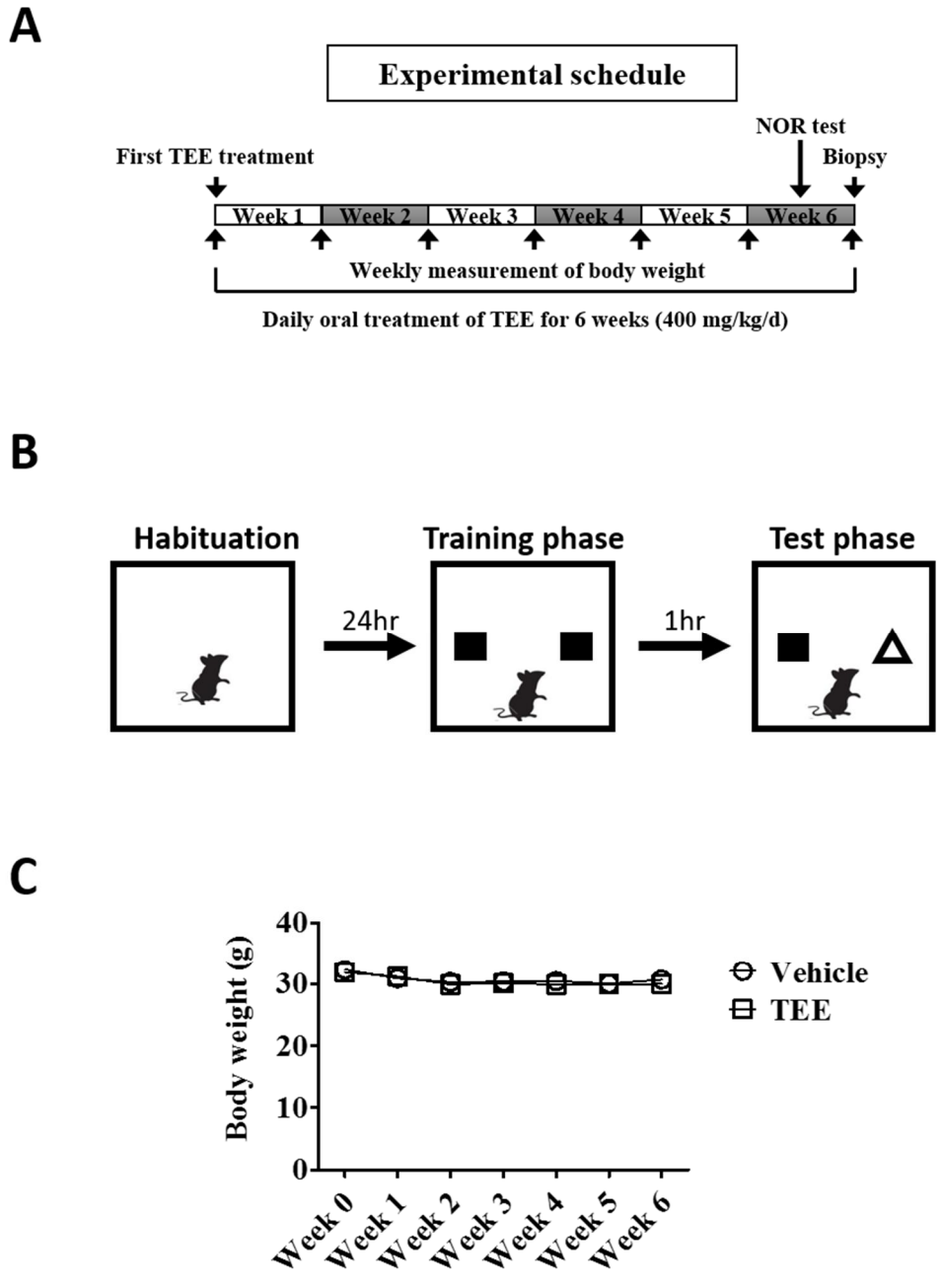
A
Experimental schedule
NOR test
First TEE treatment
Biopsy
Week 1
Week 2
Week 3
Week 4
Week 5
Week 6
Weekly measurement of body weight
Daily oral treatment of TEE for 6 weeks (400 mg/kg/d)
B
Habituation
Training phase
Test phase
24hr
1hr
C
Body weight (g)
40
30
20
10
0
Week 0
Week 1
Week 2
Week 3
Week 4
Week 5
Week 6
Vehicle
TEE

Figure 14. Study design and body weight changes of mice during the study.

(A) Experimental schedule. Vehicle or tomato ethanolic extract (TEE) was orally administered to 12-month-old aged mice once a day for 6 weeks. Two days before biopsy, the mice were subject to a novel object recognition (NOR) test. (B) Schematic representation of the NOR test protocol. On the first day, each mouse was placed in a test chamber for 5 min (habituation phase). The next day, the mouse was allowed to explore two identical objects for 5 min (training phase), followed by a 1 hr interval, and a subsequent test phase with one familiar and one novel objects for 5 min (testing phase). (C) Changes in body weight of the mice during the study. Each point represents the mean ± SEM for each group (n=9).

Figure. 15.

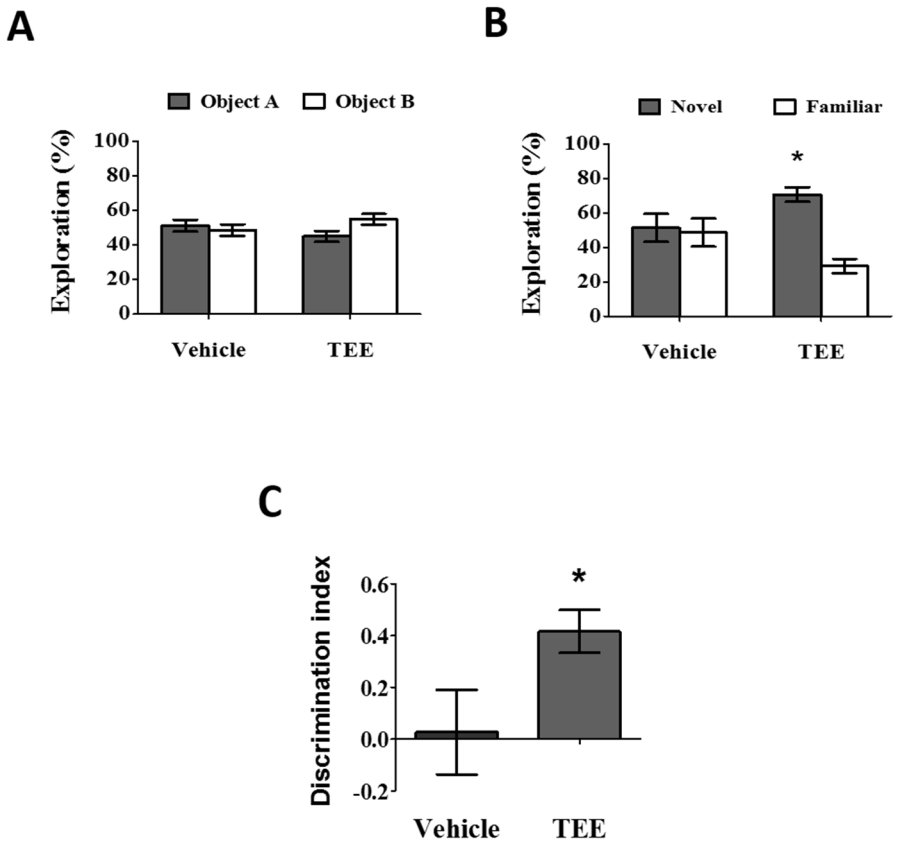
A
Object A
Object B
Exploration (%)
100
80
60
40
20
0
Vehicle
TEE
B
Novel
Familiar
Exploration (%)
*
Vehicle
TEE
C
Discrimination index
0.6
0.4
0.2
0.0
-0.2
*
Vehicle
TEE

Figure 15. Oral administration of TEE improved age-related memory impairment.

The novel object recognition test was performed to identify a preference to explore objects in the vehicle or TEE-treated mice (n=9 per group). (A) Training phase. Data are presented as the percentage of exploration time to two identical objects. (B) Test phase. Data are presented as the percentage of exploration time to a novel or familiar object. (*P<0.05, versus familiar object). (C) The discrimination index was calculated as the difference between the exploring time to novel object [N] and familiar object [F], divided by the total time exploring both objects (Discrimination index = (N-F)/(N+F). Asterisks denote a significant difference (*P<0.05, versus vehicle-treated group).

Figure. 16.

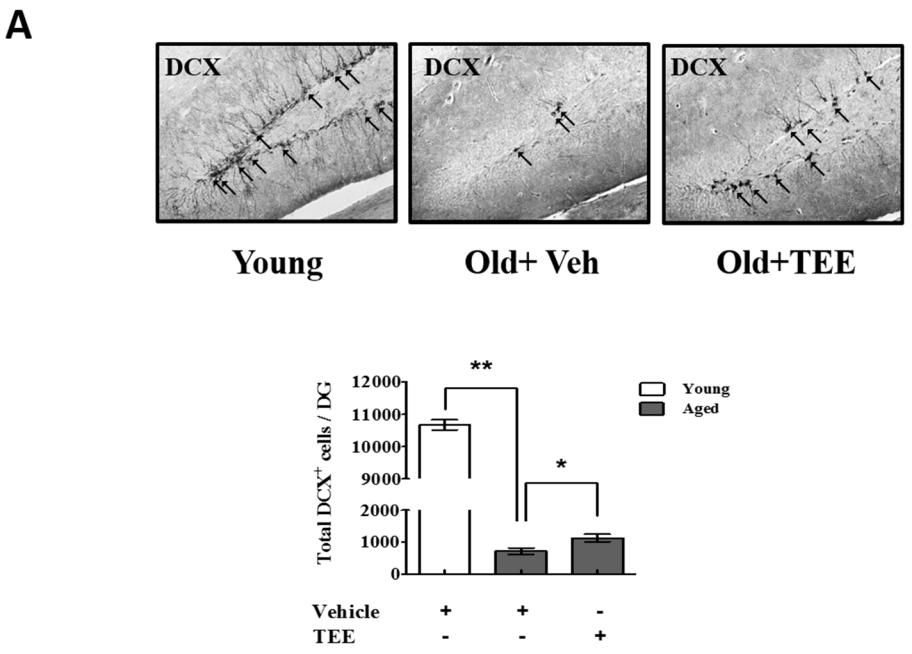
A
DCX
DCX
DCX
Young
Old+ Veh
Old+TEE
Total DCX+ cells / DG
12000
11000
10000
9000
2000
1000
0
**
*
Young
Aged
Vehicle + + -
TEE - - +
B
Young
Old+ Veh
Old+TEE
PSD95
Actin
PSD95 protein level in hippocampus(%)
150
100
50
0
***
*
Young
Aged
Vehicle + + -
TEE - - +

Figure 16. Oral administration of TEE improved hippocampal neurogenesis and synaptic density in aged mice.

(A) To quantify the neurogenesis in DG, doublecortin (DCX) immunostaining was performed. Representative photographs of DCX+ cells in the hippocampal region are shown. The arrows indicate DCX+ cells, and the total number of DCX+ cells in the DG were quantified in the graph in the lower panel. (B) The expression of PSD-95 was assessed via Western blotting. The bands shown are four representatives from each group. Relative protein expressions of PSD-95 were analyzed using the ImageJ software. The band intensity was normalized to actin. Each bar represents the mean ± SEM of each group (n=9). The asterisks denote a significant difference (*, $P < 0.05$; ***, $P < 0.001$).

Figure. 17.

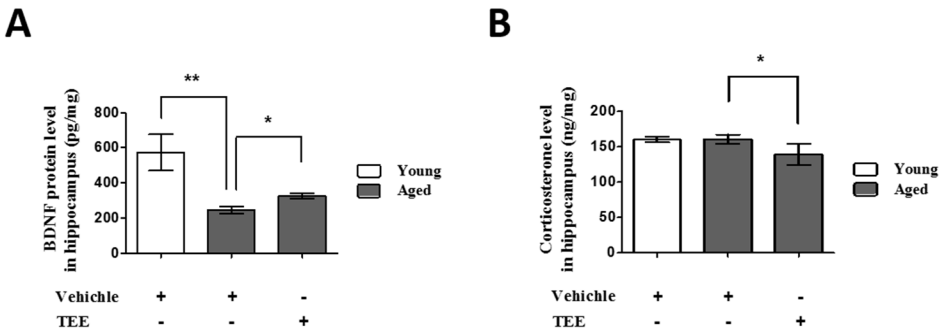

Figure 17. Oral administration of TEE decreased corticosterone and increased BDNF in in aged hippocampus.

The corticosterone (A) and BDNF (B) levels in the mouse hippocampus was measured using ELISA. Each bar represents the mean ± SEM for each group (n=9). The asterisks denote a significant difference (*, $P < 0.05$; **, $P<0.01$).

Figure. 18.

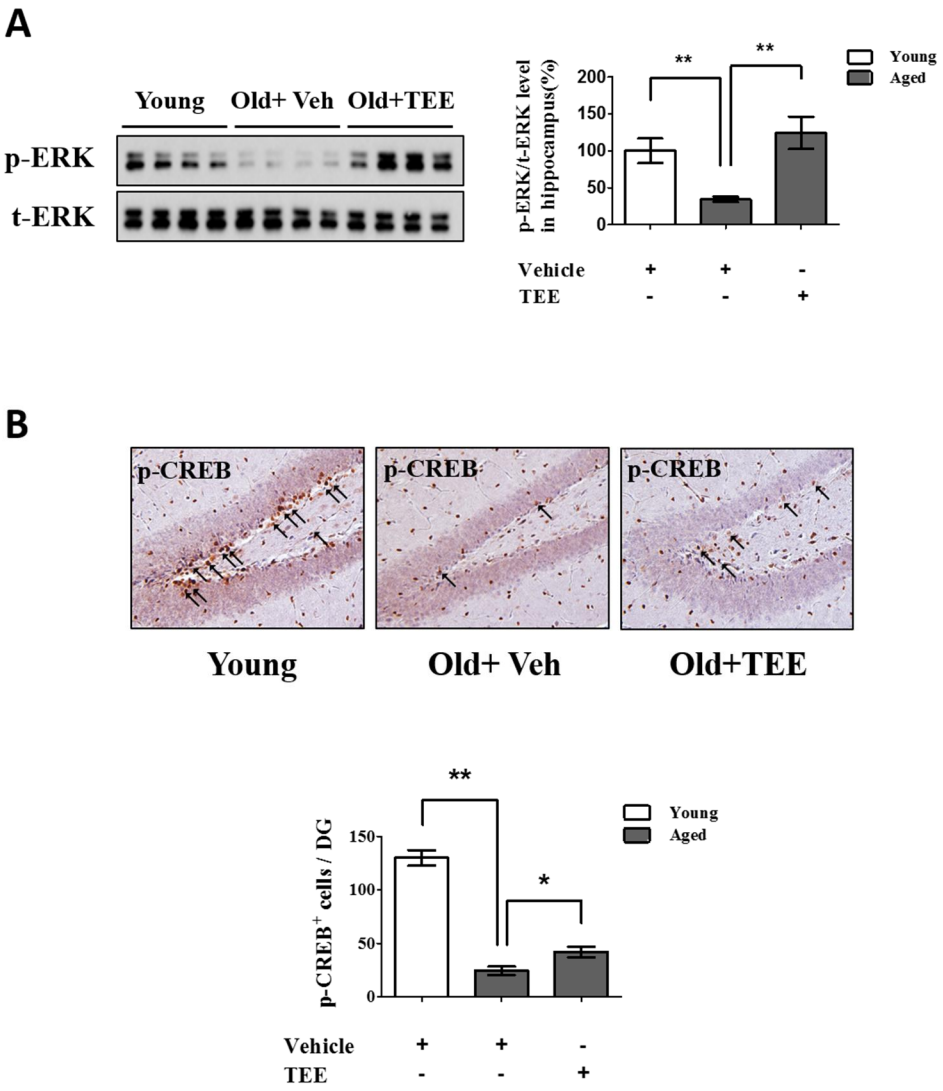
A
Young
Old+ Veh
Old+TEE
p-ERK
t-ERK
p-ERK/t-ERK level in hippocampus(%)
200
150
100
50
0
**
**
Young
Aged
Vehicle + + -
TEE - - +
B
p-CREB
p-CREB
p-CREB
Young
Old+ Veh
Old+TEE
p-CREB+ cells / DG
150
100
50
0
**
*
Young
Aged
Vehicle + + -
TEE - - +

Figure 18. Oral administration of TEE activated ERK and CREB signaling pathways in aged hippocampus.

(A) The changes in the phosphorylated form of ERK in the mice hippocampus were analyzed via Western blotting using phospho-specific ERK. The bands shown are four representatives from each group. The relative protein expressions of phospho-ERK were analyzed using the ImageJ software. The intensity of the bands was normalized to the total ERK. (B) To analyze the CREB activation in DG, phospho-CREB immunostaining was performed. Representative photographs of phospho-CREB+ cells in the hippocampal DG are shown. The arrows indicate phospho-CREB+ cells. The number of phospho-CREB+ cells in the DG was quantified in the graph in the lower panel. Each bar represents the mean ± SEM of each group (n=9). The asterisks denote a significant difference (*, $P < 0.05$; **, $P < 0.01$; ***, $P < 0.001$).

Figure. 19.

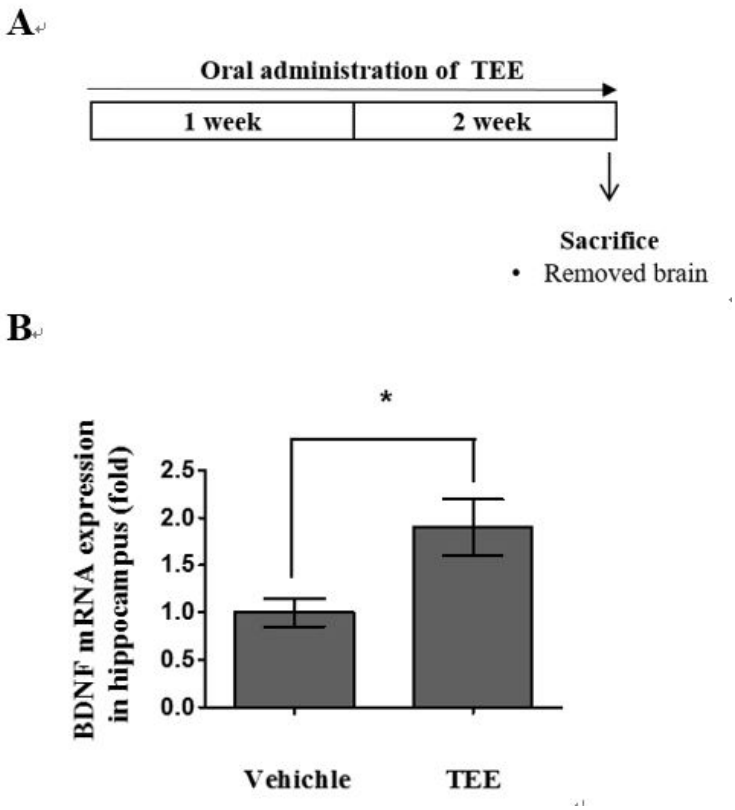
A
Oral administration of TEE
1 week
2 week
Sacrifice
• Removed brain
B
*
BDNF mRNA expression in hippocampus (fold)
2.5
2.0
1.5
1.0
0.5
0.0
Vehichle
TEE

Figure 19. Effect of TEE administration on brain-derived neurotrophic factor (BDNF) expression in the mouse brain.

(A) Schamatic design of the experiment of in vivo. Female 5weeks ICR mice were divided into two groups: vehicle and TEE. Mice were orally provided with 400 mg/kg of TEE from days 0 to 21. On last experimental day, mice were sacrificed and removed brains for hormone analysis. (B) The brain was collected and homogenized. Homogenized brain was extracted mRNA and cDNA was synthesized using the QuantiTect Reverse Transcription Kit (Qiagen). Quantification of the BDNF mRNA level by quantitative real-time RT-PCR. Expression levels were normalized to Gapdh. The expression of BDNF expression was compared between the vehicle and TEE–treated groups. Each bar represents the mean ± SEM of each group (n=6). The asterisks denote a significant difference (*, $P < 0.05$).

DISCUSSION

Over the past decade, natural ingredients from plants, vegetables, and fruits have been used for sources of pharmaceutical agents. For example, flavonoids from many kinds of plants have diverse pharmacological activities such as anti-oxidant, anti-inflammatory and anti-cancer effects [48,49]. Development of novel drugs from edible natural sources are of growing interest as fewer side effects are expected than synthetic drugs. In this study, I isolated 50% ethanolic extracts from 133 species of commonly consumed dietary plants, and performed the screening for developing anti-aging drug against skin and brain. Finally, I found out 2 species of extracts including protective effects on skin and brain aging, respectively, and elucidated their underlying mechanisms involved as well.

In chapter I, I performed the screening for agents including protective activities against photoaging and age-related cognitive decline. As targets for photoaging, UV-induced MMP-1 and -reduced procollagen were evaluated using HDFs. From the screening of western bolt analysis, I found 3 species of extracts (*P. frutescens* Leaves, *L. sativa,* and *O. sativa L*:black rice) involved in not only inhibition of UV-induced MMP-1 expression but also induction of UV-reduced procollagen expression. Finally, I decided the most effective agent,

perilla leaves, and used that for the experiment in chapter II.

For the screening for brain, I divided procedure by 3 steps as follow; (i) Finding effective peripheral neurotrophic factors, (ii) Finding agents inducing neurotrophic factors in HDFs, (iii) Finding effective agents in mice brain. I found that subcutaneous administration of BDNF, FGF-2, IGF-1 and DHEA can activate hippocampal proliferation and neuronal cell survival in Skh-1 hairless mice. HDFs were treated all extracts, and mRNA expressions of neurotrophic factors (BDNF, FGF-2 and IGF-1) were analyzed by real-time PCR. DHEA was excluded from the real-time PCR analysis since it is not protein hormone. From the screening using HDFs, 22 species of extracts were selected as agents enhancing neurotrophic factors, and 6 species (*C. longa, A. scaber, S. lycopersicum, B. oleracea, P. miliaceum* seeds, and *C.* × *limon* fruits) were used for screening using aged hairless mice. Among 6 species, *S. lycopersicum* (tomato) and *P. miliaceum* seeds (proso millet) extracts increased hippocampal neurogenesis in aged mice. Proso millet increased Ki-67 expressing cells only. However, tomato induced both Ki-67 and DCX expressing cells. Thus, I selected tomato extract, and used it for the experiment in chapter III.

In chapter II, I studied effects of *P. frutescens* leaves on UV-induced ECM damage in HDFs and SKh-1 hairless mice skin. Photo-aging is defined as premature aging of the skin induced by chronic UV exposure.

UV irradiation induces expression of MMPs resulting in the degradation of ECM protein and damage to connective tissues [8]. In recent years, many natural product-derived agents claiming anti-aging activity have been used as ingredients for skin care products. In particular, inhibitors of collagenase expression and stimulators of collagen production are considered as an effective agent against connective tissue damage associated with skin aging. In the present study, PLE decreased UV-induced MMP-1 and MMP-3 in HDFs and MMP-13 in hairless mice by inhibiting ROS production and AP-1 binding activity.

MAPK signaling pathways are involved in regulation of cellular responses to diverse stimuli, such as mitogens, heat shock, and inflammatory cytokines [50,51]. UV irradiation activates MAPK signaling cascade, leading to increased MMP-1 expression [52]. A recent study showed that lipopolysaccharide (LPS)-induced inflammation is suppressed by treatment of PLE in murine macrophages due to the inhibition of MAPK signaling pathways [53]. Similarly, PLE significantly inhibited UV-induced phosphorylation of ERK, JNK, and p-38.

UV-activated MAPK signaling triggers translocation of AP-1 into the nucleus [9,54]. Promoter binding activity of AP-1 depends on phosphorylation of c-Jun and expression of c-Fos [55]. UV irradiation

dramatically induces c-Jun phosphorylation and c-Fos expression, leading to the increased AP-1/DNA binding. However, UV-induced DNA binding of AP-1 was suppressed by PLE treatment because of the suppression of nuclear translocation of c-Fos and phospho-c-Jun.

Intracellular ROS are one of the most potent stress inducers, and are significantly provoked by UV irradiation [56,57]. UV irradiation rapidly increases intracellular hydrogen peroxide levels, which triggers the MAPK cascade. These stimuli lead to increased expression of MMP-1 and MMP-3, and eventually result in collagen breakdown. Perilla leaves have diverse biological activities by virtue of their many phenolic compounds, rosmarinic acid, anthocyanin, and vitamins, most of which are potent antioxidants [58-60]. In this study, several antioxidant compounds of PLE antioxidants including luteolin, apigenin, and rosmarinate were identified, and their photo-protective effects has been verified from previous reports. UVB-induced skin winkle formation in Skh-1 hairless mice can be significantly suppressed by the topical application of luteolin through the suppression of the JNK and p90RSK pathways [23]. Treatment of rosmarinic acid reportedly protected from DNA damage and oxidative stress in UVB-irradiated HaCaT cells [61]. Finally, it has been reported that apigenin has photochemopreventive effects on human keratinocytes [62]. Presently, PLE suppressed UV-induced ROS generation and its

downstream signaling pathway, such as MAPK signaling and AP-1. The suppression of UV-induced MMP-1 and MMP-3 expression was observed. These results indicate that antioxidant effects of PLE contribute to the suppression of UV-induced MMP-1 and MMP-3 expression.

Based on the inhibitory effects of PLE on UVB response in HDFs, further animal studies were performed to determine whether PLE also inhibited UV-induced damage *in vivo*. Changes in epidermal thickness are commonly used to evaluate UV-induced skin responses, since UV stimulates epidermal cell proliferation and epidermal hyperplasia [63]. UV-induced epidermal skin thickening was significantly reduced in UV-treated mice with PLE treatment. Furthermore, topical treatment of PLE decreased UV-induced MMP-13 expression. However, the expression of type I collagen was not changed by PLE treatment. In this study, we examined effects of PLE in acute UV-induced photo-aging mice model by one day of treatment, however, it is considered that the experimental condition is not suitable for an evaluation of collagen synthesis. In case of the treatment with optimal dose and longer time with PLE, it is possible that PLE treatment stimulates type I procollagen expression *in vivo*.

PLE effectively suppresses inflammatory responses. Oral administration of PLE produced anti-inflammatory and anti-allergenic

effects in a contact dermatitis mouse model [64]. PLE was reported to inhibit interleukin-1β--induced nitric oxide production in hepatocytes [65]. Symptoms of atopic dermatitis were also alleviated by PLE treatment in *Dermatophagoides farinae* extract-induced mouse model [66]. Since UV-induced inflammation further activates the transcription of MMPs [37], the anti-inflammatory effect of *P. frutescens* may contribute to the suppression of collagenase expression.

PLE ameliorated UV-induced ECM damage in vitro and in vivo, decreased UV-induced MMP-1 and MMP-3 expression, and increased type I collagen production in HDFs. these anti-photo-aging effects were also confirmed in UV-irradiated mice. The underlying mechanism involved in these beneficial effects could be the inhibition of ROS generation and AP-1 activation.

In chapter III, I examined effects of tomato on cognitive function in aged mice, and elucidated the underlying mechanisms involved as well. The cognitive function was evaluated using the NOR test, which is one of the most frequently used method to assess memory alterations in various subfields within neuroscience [67]. During the training session, all mice groups showed a similar preference for two identical objects. However, during the test session, the TEE-treated mice showed a significantly stronger interest in the novel object than the vehicle-

treated mice did, indicating that the TEE supplement led to a cognitive enhancement in the aged mice.

To support our behavioral test, the morphological changes and proliferation of neuronal cells in the DG were investigated via DCX immunostaining. DCX plays a critical role in promoting microtubule polymerization, and it is expressed in neuronal precursor cells and immature neurons [68]. In general, DCX protein has been used as a neurogenesis marker that is exclusively expressed in developing neurons. In our present study, the DCX expression in the DG of aged mice decreased dramatically relative to that of young mice, which is consistent with previous reports [69]. However, these reductions were partially but significantly restored by oral supplementation of TEE for 6 weeks. In addition, TEE supplementation also increased the synaptogenesis or synaptic plasticity, as shown by an increased expression of PSD95 (a postsynaptic marker). These results suggest that the cognition-enhancing effects of TEE on aged mice were a result of the activation of neuronal cell proliferation in DG.

Oral TEE treatment significantly increased the age-related reduction in BDNF expression in the hippocampus. To confirm the effect of TEE, it was investigated whether TEE enhances BDNF production in brain tissues isolated from young mice. ICR mice (female, 6 weeks) were divided two groups; vehicle-treated group and TEE-

treated group. The mice were orally administered with 400 mg/kg of TEE every day for 2 weeks. As a result, the mRNA level of BDNF in TEE-treated group was significantly increased (1.89-fold) compared with vehicle-treated group (1.0±0.37 vs. 1.89±0.73; vehicle vs. TEE) (**Figure 19**). Furthermore, the effects of TEE on the production of BDNF and NGF in astrocytes were also investigated. The treatment of TEE increased the protein level of BDNF in astrocytes, but not NGF as follows; (vehicle vs. TEE treatment, BDNF (pg/ml); 16±0 vs. 70±2). These results indicated that the administration of TEE could help to promote the development of neurogenesis and to protect the brain aging through enhancement of BDNF production.

Corticosterone levels in hippocampus were significantly decreased in the TEE-treated mice. Corticosterone is known as a stress hormone, and it is also associated with cognitive impairment [70]. Recent studies have demonstrated that increased levels of hippocampal corticosterone exhibit a poorer spatial memory performance [71], and chronic corticosterone exposure suppresses the synaptic plasticity of the mice brain [72]. Furthermore, a corticosterone treatment decreased the BDNF expression in a mouse model as well as in a hippocampal cell line [73,74]. Our results indicate that the suppression of the hippocampal corticosterone levels by TEE is also involved in the BDNF induction and cognition improvement.

BDNF is a neurotrophic factor involved neurogenesis, the modulation of synaptic plasticity, and the release of neurotransmitters [75]. BDNF-transgenic mice showed an improved cognitive function and synaptic plasticity [76] whereas BDNF knockout mice showed compromised learning and memory in spatial learning [77]. Several agents, inducing BDNF levels in the hippocampus, led to a memory enhancement in mouse models [78,79]. Moreover, an oral supplementation of TEE significantly activates the phosphorylation of ERK and CREB in the murine hippocampus. ERK1/2 is a downstream target for the BDNF signaling pathway [80], and BDNF-induced ERK activation sequentially activates the transcription factor CREB protein and neurogenic proteins that are involved in memory formation and synaptic remodeling [81]. In addition, ERK signaling is closely related with the induction and maintenance of long-term potentiation [82]. Therefore, the activation of the ERK and CREB pathway in neurons is considered to be an effective therapeutic strategy for memory impairment and related disorders. Our results indicate that the BDNF-ERK-CREB pathway is involved in the cognition-enhancing effects of TEE.

Lycopene and rutin have been known as active compounds of tomato. To reveal active components in TEE, the components in TEE were analyzed using HPLC and LC/MS. However, it was not found

high concentrated peaks, which are able to represent functionality of TEE. Case of the lycopene was included to 0.0001487% in TEE. In addition, rutin was also included to 0.00696% in TEE. These result indicated that polyphenols, flavonoids, and non-polar components reported as functional components in tomato showed low possibility as active components for functionality of TEE. Therefore, it is suggest that the enhancing effect of TEE on cognitive function via BDNF production might be derived from poly/oligo-saccharides because TEE (50% ethanolic extract of tomato) contained various hydrophilic saccharides [83,84].

Animal models with cognitive impairment have been used as a tool to evaluate cognitive functions since these reflect the complex interactions among diverse neural systems. Several new mouse models are now available with cognitive impairment induced by pharmacologic, toxicological, and genetic methods [85]. Although these animal models have been successfully applied to investigate memory disorders, such as Alzheimer's disease [86] and PD [87], the age-related cognitive decline is not fully explained using these artificially-induced models. Although a relatively longer time and additional resources are needed to use naturally-aged mice, naturally-aged mice were employed to recapitulate the aging systemic milieu [88] and subsequent response to TEE supplementation.

In this study, it is observed that an oral administration of TEE for 6 weeks enhanced cognition in aged mice. The TEE supplement improved the age-related reduction of hippocampal neurogenesis, increased BDNF production, and increased the levels of phosphorylated ERK and CREB in the hippocampus. Taken together, the cognition-enhancing effect of TEE might be attributed to increased neurogenesis and synapse formation in the hippocampus via activation of the BDNF signaling pathway.

In summary, I demonstrated the potential of several putative agents for protection skin and brain aging in chapter I. And, perilla leaves and tomato were selected as the most effective extracts on skin and brain, respectively. The results in chapter II suggest that PLE is a potential natural product for prevention and treatment of skin aging by inhibiting the ROS generation and AP-1 activation. Furthermore, the results in chapter III suggest that TEE can be a potential candidate to treat age-related memory impairment and neurodegenerative disorders. Furthermore, it is suggested that increased consumption of tomato (salad or tomato-based food) would contribute to protect against brain aging.

REFERENCES

1. Kohl, E.; Steinbauer, J.; Landthaler, M.; Szeimies, R.M. Skin ageing. *J. Eur. Acad. Dermatol. Venereol.* **2011**, *25*, 873-884.

2. Sternlicht, M.D.; Werb, Z. How matrix metalloproteinases regulate cell behavior. *Annu. Rev. Cell Dev. Biol.* **2001**, *17*, 463-516.

3. Chen, Q.; Jin, M.; Yang, F.; Zhu, J.; Xiao, Q.; Zhang, L. Matrix metalloproteinases: Inflammatory regulators of cell behaviors in vascular formation and remodeling. *Mediators Inflamm.* **2013**, *2013*, 928315.

4. Manon-Jensen, T.; Kjeld, N.G.; Karsdal, M.A. Collagen-mediated hemostasis. *J. Thromb. Haemost.* **2016**, *14*, 438-448.

5. Quan, T.; Qin, Z.; Xia, W.; Shao, Y.; Voorhees, J.J.; Fisher, G.J. Matrix-degrading metalloproteinases in photoaging. *J. Investig. Dermatol. Symp. Proc.* **2009**, *14*, 20-24.

6. Lam, P.Y.; Yan, C.W.; Chiu, P.Y.; Leung, H.Y.; Ko, K.M. Schisandrin b protects against solar irradiation-induced oxidative stress in rat skin tissue. *Fitoterapia* **2011**, *82*, 393-400.

7. Chen, C.C.; Chiang, A.N.; Liu, H.N.; Chang, Y.T. Egb-761 prevents ultraviolet b-induced photoaging via inactivation of mitogen-activated protein kinases and proinflammatory cytokine expression. *J. Dermatol. Sci.* **2014**, *75*, 55-62.

8. Fisher, G.J.; Kang, S.; Varani, J.; Bata-Csorgo, Z.; Wan, Y.; Datta, S.; Voorhees, J.J. Mechanisms of photoaging and chronological skin aging. *Arch. Dermatol.* **2002**, *138*, 1462-1470.

9. Karin, M. The regulation of ap-1 activity by mitogen-activated protein kinases. *J. Biol. Chem.* **1995**, *270*, 16483-16486.

10. Lazarov, O.; Hollands, C. Hippocampal neurogenesis: Learning to remember. *Prog Neurobiol* **2016**.

11. Riddle, D.R.; Lichtenwalner, R.J. Neurogenesis in the adult and aging brain. In *Brain aging: Models, methods, and mechanisms*, Riddle, D.R., Ed. Boca Raton (FL), 2007.

12. Hung, C.W.; Chen, Y.C.; Hsieh, W.L.; Chiou, S.H.; Kao, C.L. Ageing and neurodegenerative diseases. *Ageing Res Rev* **2010**, *9 Suppl 1*, S36-46.

13. Seib, D.R.; Martin-Villalba, A. Neurogenesis in the normal ageing hippocampus: A mini-review. *Gerontology* **2015**, *61*, 327-335.

14. Driscoll, I.; Hamilton, D.A.; Petropoulos, H.; Yeo, R.A.; Brooks, W.M.; Baumgartner, R.N.; Sutherland, R.J. The aging hippocampus: Cognitive, biochemical and structural findings. *Cereb Cortex* **2003**, *13*, 1344-1351.

15. Lee, E.; Son, H. Adult hippocampal neurogenesis and related neurotrophic factors. *BMB Rep* **2009**, *42*, 239-244.

16. Lim, S.; Moon, M.; Oh, H.; Kim, H.G.; Kim, S.Y.; Oh, M.S.

Ginger improves cognitive function via ngf-induced erk/creb activation in the hippocampus of the mouse. *J Nutr Biochem* **2014**, *25*, 1058-1065.

17. Xiang, J.; Pan, J.; Chen, F.; Zheng, L.; Chen, Y.; Zhang, S.; Feng, W. L-3-n-butylphthalide improves cognitive impairment of app/ps1 mice by bdnf/trkb/pi3k/akt pathway. *International journal of clinical and experimental medicine* **2014**, *7*, 1706-1713.

18. Park, H.; Poo, M.M. Neurotrophin regulation of neural circuit development and function. *Nat Rev Neurosci* **2013**, *14*, 7-23.

19. Jiang, P.; Zhu, T.; Xia, Z.; Gao, F.; Gu, W.; Chen, X.; Yuan, T.; Yu, H. Inhibition of mapk/erk signaling blocks hippocampal neurogenesis and impairs cognitive performance in prenatally infected neonatal rats. *Eur Arch Psychiatry Clin Neurosci* **2015**, *265*, 497-509.

20. Bae, J.S.; Han, M.; Yao, C.; Chung, J.H. Chaetocin inhibits ibmx-induced melanogenesis in b16f10 mouse melanoma cells through activation of erk. *Chem. Biol. Interact.* **2016**, *245*, 66-71.

21. Lan, C.C.; Wu, C.S.; Yu, H.S. Solar-simulated radiation and heat treatment induced metalloproteinase-1 expression in cultured dermal fibroblasts via distinct pathways: Implications on reduction of sun-associated aging. *J. Dermatol. Sci.* **2013**, *72*, 290-295.

22. Banno, N.; Akihisa, T.; Tokuda, H.; Yasukawa, K.; Higashihara, H.; Ukiya, M.; Watanabe, K.; Kimura, Y.; Hasegawa, J.; Nishino, H. Triterpene acids from the leaves of perilla frutescens and their anti-

inflammatory and antitumor-promoting effects. *Biosci Biotechnol Biochem* **2004**, *68*, 85-90.

23. Lim, S.H.; Jung, S.K.; Byun, S.; Lee, E.J.; Hwang, J.A.; Seo, S.G.; Kim, Y.A.; Yu, J.G.; Lee, K.W.; Lee, H.J. Luteolin suppresses uvb-induced photoageing by targeting jnk1 and p90 rsk2. *J Cell Mol Med* **2013**, *17*, 672-680.

24. Jeon, I.H.; Kim, H.S.; Kang, H.J.; Lee, H.S.; Jeong, S.I.; Kim, S.J.; Jang, S.I. Anti-inflammatory and antipruritic effects of luteolin from perilla (p. Frutescens l.) leaves. *Molecules* **2014**, *19*, 6941-6951.

25. Takeda, H.; Tsuji, M.; Matsumiya, T.; Kubo, M. Identification of rosmarinic acid as a novel antidepressive substance in the leaves of perilla frutescens britton var. Acuta kudo (perillae herba). *Nihon Shinkei Seishin Yakurigaku Zasshi* **2002**, *22*, 15-22.

26. Deng, Y.M.; Xie, Q.M.; Zhang, S.J.; Yao, H.Y.; Zhang, H. Anti-asthmatic effects of perilla seed oil in the guinea pig in vitro and in vivo. *Planta Med* **2007**, *73*, 53-58.

27. Chen, C.Y.; Leu, Y.L.; Fang, Y.; Lin, C.F.; Kuo, L.M.; Sung, W.C.; Tsai, Y.F.; Chung, P.J.; Lee, M.C.; Kuo, Y.T., *et al.* Anti-inflammatory effects of perilla frutescens in activated human neutrophils through two independent pathways: Src family kinases and calcium. *Sci. Rep.* **2015**, *5*, 18204.

28. Huang, B.P.; Lin, C.H.; Chen, Y.C.; Kao, S.H. Anti-

inflammatory effects of perilla frutescens leaf extract on lipopolysaccharide-stimulated raw264.7 cells. *Mol Med Rep* **2014**, *10*, 1077-1083.

29. Urushima, H.; Nishimura, J.; Mizushima, T.; Hayashi, N.; Maeda, K.; Ito, T. Perilla frutescens extract ameliorates dss-induced colitis by suppressing proinflammatory cytokines and inducing anti-inflammatory cytokines. *Am J Physiol Gastrointest Liver Physiol* **2015**, *308*, G32-41.

30. Kim, M.J.; Kim, H.K. Perilla leaf extract ameliorates obesity and dyslipidemia induced by high-fat diet. *Phytotherapy research : PTR* **2009**, *23*, 1685-1690.

31. Park, C.H.; Lee, M.J.; Kim, J.P.; Yoo, I.D.; Chung, J.H. Prevention of uv radiation-induced premature skin aging in hairless mice by the novel compound melanocin a. *Photochem. Photobiol.* **2006**, *82*, 574-578.

32. Shin, J.E.; Oh, J.H.; Kim, Y.K.; Jung, J.Y.; Chung, J.H. Transcriptional regulation of proteoglycans and glycosaminoglycan chain-synthesizing glycosyltransferases by uv irradiation in cultured human dermal fibroblasts. *J. Korean Med. Sci.* **2011**, *26*, 417-424.

33. Meng, L.; Lozano, Y.; Bombarda, I.; Gaydou, E.; Li, B. Anthocyanin and flavonoid production from perilla frutescens: Pilot plant scale processing including cross-flow microfiltration and reverse

osmosis. *J Agric Food Chem* **2006**, *54*, 4297-4303.

34. Linghua Meng, Y.L., Isabelle Bombarda, Emile M. Gaydou, Bin Li. Polyphenol extraction from eight perilla frutescens cultivars. *Comptes Rendus Chimie* **2009**, *Volume 12*, 602–611.

35. Kim, M.K.; Lee, S.; Kim, E.J.; Kong, K.H.; Lee, D.H.; Chung, J.H. Topical application of anacardic acid (6-nonadecyl salicylic acid) reduces uv-induced histone modification, mmp-13, mmp-9, cox-2 and tnf-alpha expressions in hairless mice skin. *J. Dermatol. Sci.* **2013**, *70*, 64-67.

36. Kim, J.M.; Noh, E.M.; Kwon, K.B.; Hwang, B.M.; Hwang, J.K.; You, Y.O.; Kim, M.S.; Lee, W.; Lee, J.H.; Kim, H.J.*, et al.* Dihydroavenanthramide d prevents uv-irradiated generation of reactive oxygen species and expression of matrix metalloproteinase-1 and -3 in human dermal fibroblasts. *Exp. Dermatol.* **2013**, *22*, 759-761.

37. Pillai, S.; Oresajo, C.; Hayward, J. Ultraviolet radiation and skin aging: Roles of reactive oxygen species, inflammation and protease activation, and strategies for prevention of inflammation-induced matrix degradation - a review. *Int J Cosmet Sci* **2005**, *27*, 17-34.

38. Ilic, D.; Forbes, K.M.; Hassed, C. Lycopene for the prevention of prostate cancer. *Cochrane Database Syst Rev* **2011**, CD008007.

39. Hung, C.F.; Huang, T.F.; Chen, B.H.; Shieh, J.M.; Wu, P.H.; Wu, W.B. Lycopene inhibits tnf-alpha-induced endothelial icam-1

expression and monocyte-endothelial adhesion. *Eur J Pharmacol* **2008**, *586*, 275-282.

40. Ghavipour, M.; Saedisomeolia, A.; Djalali, M.; Sotoudeh, G.; Eshraghyan, M.R.; Moghadam, A.M.; Wood, L.G. Tomato juice consumption reduces systemic inflammation in overweight and obese females. *Br J Nutr* **2013**, *109*, 2031-2035.

41. di Matteo, V.; Pierucci, M.; Di Giovanni, G.; Dragani, L.K.; Murzilli, S.; Poggi, A.; Esposito, E. Intake of tomato-enriched diet protects from 6-hydroxydopamine-induced degeneration of rat nigral dopaminergic neurons. *J Neural Transm Suppl* **2009**, 333-341.

42. Gokul, K.; Muralidhara. Oral supplements of aqueous extract of tomato seeds alleviate motor abnormality, oxidative impairments and neurotoxicity induced by rotenone in mice: Relevance to parkinson's disease. *Neurochem Res* **2014**, *39*, 1382-1394.

43. Prema, A.; Janakiraman, U.; Manivasagam, T.; Thenmozhi, A.J. Neuroprotective effect of lycopene against mptp induced experimental parkinson's disease in mice. *Neurosci Lett* **2015**, *599*, 12-19.

44. Antunes, M.; Biala, G. The novel object recognition memory: Neurobiology, test procedure, and its modifications. *Cogn Process* **2012**, *13*, 93-110.

45. Bae, J.S.; Park, H.S.; Park, J.W.; Li, S.H.; Chun, Y.S. Red ginseng and 20(s)-rg3 control testosterone-induced prostate hyperplasia

by deregulating androgen receptor signaling. *J Nat Med* **2012**, *66*, 476-485.

46. Jacobsen, J.P.; Mork, A. Chronic corticosterone decreases brain-derived neurotrophic factor (bdnf) mrna and protein in the hippocampus, but not in the frontal cortex, of the rat. *Brain Res* **2006**, *1110*, 221-225.

47. Murray, P.S.; Holmes, P.V. An overview of brain-derived neurotrophic factor and implications for excitotoxic vulnerability in the hippocampus. *Int J Pept* **2011**, *2011*, 654085.

48. Romagnolo, D.F.; Selmin, O.I. Flavonoids and cancer prevention: A review of the evidence. *J Nutr Gerontol Geriatr* **2012**, *31*, 206-238.

49. Nijveldt, R.J.; van Nood, E.; van Hoorn, D.E.; Boelens, P.G.; van Norren, K.; van Leeuwen, P.A. Flavonoids: A review of probable mechanisms of action and potential applications. *Am J Clin Nutr* **2001**, *74*, 418-425.

50. Raingeaud, J.; Gupta, S.; Rogers, J.S.; Dickens, M.; Han, J.; Ulevitch, R.J.; Davis, R.J. Pro-inflammatory cytokines and environmental stress cause p38 mitogen-activated protein kinase activation by dual phosphorylation on tyrosine and threonine. *J. Biol. Chem.* **1995**, *270*, 7420-7426.

51. Denton, C.P.; Black, C.M.; Abraham, D.J. Mechanisms and

consequences of fibrosis in systemic sclerosis. *Nat. Clin. Pract. Rheumatol.* **2006**, *2*, 134-144.

52. Wang, X.; Bi, Z.; Chu, W.; Wan, Y. Il-1 receptor antagonist attenuates map kinase/ap-1 activation and mmp1 expression in uva-irradiated human fibroblasts induced by culture medium from uvb-irradiated human skin keratinocytes. *Int J Mol Med* **2005**, *16*, 1117-1124.

53. Lee, H.A.; Han, J.S. Anti-inflammatory effect of perilla frutescens (l.) britton var. Frutescens extract in lps-stimulated raw 264.7 macrophages. *Prev Nutr Food Sci* **2012**, *17*, 109-115.

54. Kim, H.H.; Shin, C.M.; Park, C.H.; Kim, K.H.; Cho, K.H.; Eun, H.C.; Chung, J.H. Eicosapentaenoic acid inhibits uv-induced mmp-1 expression in human dermal fibroblasts. *J. Lipid Res.* **2005**, *46*, 1712-1720.

55. Uluckan, O.; Guinea-Viniegra, J.; Jimenez, M.; Wagner, E.F. Signalling in inflammatory skin disease by ap-1 (fos/jun). *Clin. Exp. Rheumatol.* **2015**, *33*, S44-49.

56. Bond, M.; Baker, A.H.; Newby, A.C. Nuclear factor kappab activity is essential for matrix metalloproteinase-1 and -3 upregulation in rabbit dermal fibroblasts. *Biochem. Biophys. Res. Commun.* **1999**, *264*, 561-567.

57. Rinnerthaler, M.; Bischof, J.; Streubel, M.K.; Trost, A.; Richter,

K. Oxidative stress in aging human skin. *Biomolecules* **2015**, *5*, 545-589.

58. Asif, M. Phytochemical study of polyphenols in perilla frutescens as an antioxidant. *Avicenna J Phytomed* **2012**, *2*, 169-178.

59. Jun, H.I.; Kim, B.T.; Song, G.S.; Kim, Y.S. Structural characterization of phenolic antioxidants from purple perilla (perilla frutescens var. Acuta) leaves. *Food Chem.* **2014**, *148*, 367-372.

60. Meng, L.; Metro, D.G.; Patel, R.M. Evaluating professionalism and interpersonal and communication skills: Implementing a 360-degree evaluation instrument in an anesthesiology residency program. *J Grad Med Educ* **2009**, *1*, 216-220.

61. Vostalova, J.; Zdarilova, A.; Svobodova, A. Prunella vulgaris extract and rosmarinic acid prevent uvb-induced DNA damage and oxidative stress in hacat keratinocytes. *Arch Dermatol Res* **2010**, *302*, 171-181.

62. Abu-Yousif, A.O.; Smith, K.A.; Getsios, S.; Green, K.J.; Van Dross, R.T.; Pelling, J.C. Enhancement of uvb-induced apoptosis by apigenin in human keratinocytes and organotypic keratinocyte cultures. *Cancer Res* **2008**, *68*, 3057-3065.

63. Lee, Y.M.; Kang, S.M.; Lee, S.R.; Kong, K.H.; Lee, J.Y.; Kim, E.J.; Chung, J.H. Inhibitory effects of trpv1 blocker on uv-induced responses in the hairless mice. *Arch. Dermatol. Res.* **2011**, *303*, 727-

736.

64. Ueda, H.; Yamazaki, M. Anti-inflammatory and anti-allergic actions by oral administration of a perilla leaf extract in mice. *Biosci. Biotechnol. Biochem.* **2001**, *65*, 1673-1675.

65. Nakajima, A.; Yamamoto, Y.; Yoshinaka, N.; Namba, M.; Matsuo, H.; Okuyama, T.; Yoshigai, E.; Okumura, T.; Nishizawa, M.; Ikeya, Y. A new flavanone and other flavonoids from green perilla leaf extract inhibit nitric oxide production in interleukin 1beta-treated hepatocytes. *Biosci. Biotechnol. Biochem.* **2015**, *79*, 138-146.

66. Komatsu, K.I.; Takanari, J.; Maeda, T.; Kitadate, K.; Sato, T.; Mihara, Y.; Uehara, K.; Wakame, K. Perilla leaf extract prevents atopic dermatitis induced by an extract of dermatophagoides farinae in nc/nga mice. *Asian Pac. J. Allergy Immunol.* **2016**.

67. Moore, S.J.; Deshpande, K.; Stinnett, G.S.; Seasholtz, A.F.; Murphy, G.G. Conversion of short-term to long-term memory in the novel object recognition paradigm. *Neurobiol Learn Mem* **2013**, *105*, 174-185.

68. Ramirez-Rodriguez, G.; Ortiz-Lopez, L.; Dominguez-Alonso, A.; Benitez-King, G.A.; Kempermann, G. Chronic treatment with melatonin stimulates dendrite maturation and complexity in adult hippocampal neurogenesis of mice. *J Pineal Res* **2011**, *50*, 29-37.

69. Kuipers, S.D.; Schroeder, J.E.; Trentani, A. Changes in

hippocampal neurogenesis throughout early development. *Neurobiology of aging* **2015**, *36*, 365-379.

70. Brummelte, S.; Galea, L.A. Chronic high corticosterone reduces neurogenesis in the dentate gyrus of adult male and female rats. *Neuroscience* **2010**, *168*, 680-690.

71. Tronche, C.; Pierard, C.; Coutan, M.; Chauveau, F.; Liscia, P.; Beracochea, D. Increased stress-induced intra-hippocampus corticosterone rise associated with memory impairments in middle-aged mice. *Neurobiology of learning and memory* **2010**, *93*, 343-351.

72. Zhang, H.; Zhao, Y.; Wang, Z. Chronic corticosterone exposure reduces hippocampal astrocyte structural plasticity and induces hippocampal atrophy in mice. *Neuroscience letters* **2015**, *592*, 76-81.

73. Hansson, A.C.; Sommer, W.H.; Metsis, M.; Stromberg, I.; Agnati, L.F.; Fuxe, K. Corticosterone actions on the hippocampal brain-derived neurotrophic factor expression are mediated by exon iv promoter. *Journal of neuroendocrinology* **2006**, *18*, 104-114.

74. Yu, I.T.; Lee, S.H.; Lee, Y.S.; Son, H. Differential effects of corticosterone and dexamethasone on hippocampal neurogenesis in vitro. *Biochemical and biophysical research communications* **2004**, *317*, 484-490.

75. Harrisberger, F.; Smieskova, R.; Schmidt, A.; Lenz, C.; Walter, A.; Wittfeld, K.; Grabe, H.J.; Lang, U.E.; Fusar-Poli, P.; Borgwardt, S.

Bdnf val66met polymorphism and hippocampal volume in neuropsychiatric disorders: A systematic review and meta-analysis. *Neurosci Biobehav Rev* **2015**, *55*, 107-118.

76. Tolwani, R.J.; Buckmaster, P.S.; Varma, S.; Cosgaya, J.M.; Wu, Y.; Suri, C.; Shooter, E.M. Bdnf overexpression increases dendrite complexity in hippocampal dentate gyrus. *Neuroscience* **2002**, *114*, 795-805.

77. Gorski, J.A.; Balogh, S.A.; Wehner, J.M.; Jones, K.R. Learning deficits in forebrain-restricted brain-derived neurotrophic factor mutant mice. *Neuroscience* **2003**, *121*, 341-354.

78. Katoh-Semba, R.; Asano, T.; Ueda, H.; Morishita, R.; Takeuchi, I.K.; Inaguma, Y.; Kato, K. Riluzole enhances expression of brain-derived neurotrophic factor with consequent proliferation of granule precursor cells in the rat hippocampus. *FASEB journal : official publication of the Federation of American Societies for Experimental Biology* **2002**, *16*, 1328-1330.

79. Lee, J.S.; Kim, H.G.; Lee, H.W.; Han, J.M.; Lee, S.K.; Kim, D.W.; Saravanakumar, A.; Son, C.G. Hippocampal memory enhancing activity of pine needle extract against scopolamine-induced amnesia in a mouse model. *Scientific reports* **2015**, *5*, 9651.

80. Hutchison, M.R. Bdnf alters erk/p38 mapk activity ratios to promote differentiation in growth plate chondrocytes. *Molecular*

endocrinology **2012**, *26*, 1406-1416.

81. Vaynman, S.; Ying, Z.; Gomez-Pinilla, F. Hippocampal bdnf mediates the efficacy of exercise on synaptic plasticity and cognition. *The European journal of neuroscience* **2004**, *20*, 2580-2590.

82. Winder, D.G.; Martin, K.C.; Muzzio, I.A.; Rohrer, D.; Chruscinski, A.; Kobilka, B.; Kandel, E.R. Erk plays a regulatory role in induction of ltp by theta frequency stimulation and its modulation by beta-adrenergic receptors. *Neuron* **1999**, *24*, 715-726.

83. Jia, S.; Lu, Z.; Gao, Z.; An, J.; Wu, X.; Li, X.; Dai, X.; Zheng, Q.; Sun, Y. Chitosan oligosaccharides alleviate cognitive deficits in an amyloid-beta1-42-induced rat model of alzheimer's disease. *Int J Biol Macromol* **2016**, *83*, 416-425.

84. Yen, C.H.; Wang, C.H.; Wu, W.T.; Chen, H.L. Fructo-oligosaccharide improved brain beta-amyloid, beta-secretase, cognitive function, and plasma antioxidant levels in d-galactose-treated balb/cj mice. *Nutr Neurosci* **2015**.

85. Levin, E.D.; Buccafusco, J.J. *Animal models of cognitive impairment*. CRC/Taylor & Francis: Boca Raton, 2006; p 376 p.

86. Kloskowska, E.; Pham, T.M.; Nilsson, T.; Zhu, S.; Oberg, J.; Codita, A.; Pedersen, L.A.; Pedersen, J.T.; Malkiewicz, K.; Winblad, B., *et al.* Cognitive impairment in the tg6590 transgenic rat model of alzheimer's disease. *Journal of cellular and molecular medicine* **2010**,

14, 1816-1823.

87. Kumar, P.; Kaundal, R.K.; More, S.; Sharma, S.S. Beneficial effects of pioglitazone on cognitive impairment in mptp model of parkinson's disease. *Behavioural brain research* **2009**, *197*, 398-403.

88. Villeda, S.A.; Luo, J.; Mosher, K.I.; Zou, B.; Britschgi, M.; Bieri, G.; Stan, T.M.; Fainberg, N.; Ding, Z.; Eggel, A.*, et al.* The ageing systemic milieu negatively regulates neurogenesis and cognitive function. *Nature* **2011**, *477*, 90-94.

국 문 초 록

노화란 살아있는 생명체에게서 시간에 지남에 따라 일어나는 자연스러운 현상이다. 노화가 일어나면서 신체에는 외적, 내적인 변화를 겪는다. 이러한 현상은 노화로 인한 신체를 구성하는 각종 장기들의 기능이 떨어지기 때문이라고 잘 알려져 있다. 노화에 의한 외적인 변화 중 가장 우선적인 변화는 피부부터 일어난다. 가장 두드러진 피부의 노화현상은 주름이다. 주름은 노화에 따른 진피내의 세포 외 기질단백질의 분해에 의하여 일어난다고 잘 알려져 있다. 또 다른 피부의 변화로는 수분 보유능력의 저하로써 피부의 장벽기능이 약해져서 나타나는 현상이다. 노화의 의해 영향을 받는 조직 중 뇌 또한 노화의 영향을 가장 많이 받는다고 알려져 있다. 현재 많은 노인들이 기억력 감소에 따른 인지기능 장애를 겪고 있으며, 이러한 현상의 원인으로 나이가 들면서 뇌신경세포를 촉진시키는 성장인자들이 감소하며, 이에 따른 신경세포 증식 감소하기 때문이라는 보고가 있다.

최근 들어 노화에 대한 관심이 높아지고 지고 있으며, 이러한 노화를 억제하게 위한 여러 노력이 이루어지고 있다. 본 실험에서는 이러한 피부와 뇌기능의 노화를 감소시키는 물질을 찾는 것에 그 목적을 두고 있다. Chapter I 에서는 이러한 물질의 후보로써 135개의 다소비 식품 (식물) 로부터 50% 에탄올 주정을 획득 하였고, 세포실험 및 동물실험을 이용하여 노화를 억제 할 수 있는 물질을 찾으려는 노력을 하였다. 총 135개 효능물질 탐색을 통하여 효능물질을 탐색하였고 최종적으로 피부의 광노화 및 노인성 뇌기능 저하를

억제하는 물질을 각각 1종씩 발굴하였다.

Chapter II 에서는 자외선에 의해 유도된 ECM 손상에 대한 들깻잎 추출물의 효능을 확인하는 실험으로, 피부 유래 섬유아세포 및 무모쥐를 이용한 실험을 통하여 그 효능을 평가하였다. 실험결과, 들깻잎 추출물 처리에 의해 MMP-1 의 발현이 농도의존적으로 감소되는 것이 확인 되었으며, ERK 및 JNK 의 인산화 감소 또한 확인 되었다. 이러한 ERK 와 JNK 인산화의 감소는 c-Jun 인산화와 c-Fos 의 발현을 순차적으로 감소를 시키며 최종적으로 AP-1 DNA binding activity 를 억제하는 것으로 확인되었다. 또한 기전연구를 통하여 들깻잎의 MMP-1 발현 억제효과가 자외선 조사에 의해 발생되는 ROS 를 감소에 의한 것이라는 것을 증명하였다. 자외선을 이용한 무모쥐의 광노화 모델을 이용한 들깻잎 추출물의 피부도포 실험에서 들깻잎의 MMP-1, MMP-3 의 감소효과를 MMP-13 을 통하여 다시 한번 증명하였으며, 자외선에 의해 증가된 표피층의 증가 또한 감소되는 것도 확인 하였다. 하지만 type I procollagen 의 발현변화는 크게 나타나지 않았다.

결론적으로 본 실험에서는 세포 및 동물실험을 통하여 들깻잎의 광노화 억제 효과를 증명하였으며, 이러한 들깻잎이 광노화를 억제하는 물질로써 더욱 발전되고 활용될 것이라 기대한다.

Chapter III 에서는 토마토 추출물에 의한 노화된 쥐의 감소된 기억력 억제 및 신경세포 증진효과를 보는 실험을 진행하였다. 토마토는 전세계적으로 널리 섭취되고 과일로써 polyphenols 및

flavonoids 등의 생리활성 물질을 많이 함유되어 있다. 본 실험에서는 이러한 토마토가 인지기능에도 효과가 있는지 실험을 수행하였으며, 12개월 된 노화된 인지기능이 저하된 쥐를 이용하여 이러한 효과에 연관된 기전 또한 살펴보았다.

총 3개의 동물군을 설정하여 인지기능을 수행하였으며, 주 5회 총 6주간의 경구투여를 실시하였다. 동물군은 젊은 쥐, 노화된 쥐+, 노화된 쥐+토마토 추출물 처리 군으로 구성되었다. 수행된 인지기능 행동실험은 신물질탐색시험 (NOR test) 이었으며, 이 시험의 결과 토마토를 6주간 경구투여를 한 노화 쥐에서 교체된 새로운 물체에 관심을 갖는 시간이 추출물을 처리하지 않은 노화 쥐에 비하여 유의적으로 높았으며, 인지기능을 측정하는 척도인 discrimination index 또한 더 높게 나왔다. 또한 DCX 면역염색을 통하여, 토마토 추출물을 처리한 쥐의 해마의 신경세포의 증식이 일어난 것을 확인하였으며, 더불어 시냅스의 양을 나타내는 마커인 PSG95 역시 증가되어 있음을 확인하였다. 기전연구에서는 토마토의 이러한 효과들이 뇌 해마의 BDNF 양의 증가 및 이에 따른 ERK /CREB signaling pathway 를 활성화와 뇌 해마의 corticosterone 양의 감소에 의한 것임이 증명하였다.

결론적으로 본 실험에서는 토마토 추출물의 노화 쥐로부터 인지기능의 증가효과를 보인다는 것을 증명하였으며 이러한 효과는 BDNF 관련 signaling 의 활성화를 통한 해마의 신경세포 분화 및 시

냅스의 양이 증가 하기 때문임을 확인하였다. 때문에 우리는 토마토 추출물이 나아가 노화에 의한 기억적 감소나 신경퇴행성질환의 치료제로써 발전되고 이용될 것이라 기대한다.